The Pennsylvania State University
The Graduate School
Department of Civil and Environmental Engineering

NOVEL PERFORMANCE TESTS FOR EVALUATION OF ALKALI-SILICA REACTION

A Thesis in
Civil Engineering
by
Stephen B. Salwocki

Submitted in Partial Fulfillment
of the Requirements
for the Degree of

Master of Science

May 2016

The thesis of Stephen Salwocki was reviewed and approved* by the following:

Farshad Rajabipour
Associate Professor in Civil and Environmental Engineering
Thesis Advisor

Ali Memari
Professor in Civil and Environmental Engineering
Bernard and Henrietta Hankin Chair of Residential Construction

William Burgos
Professor in Civil and Environmental Engineering
Graduate Officer-Department of Civil and Environmental Engineering

*Signatures are on file in the Graduate School

ABSTRACT

Alkali-silica reaction (ASR) is a leading cause of premature concrete deterioration, resulting in cracks that develop in concrete structures. ASR is a slow chemical reaction, taking years to manifest. Therefore, ASTM currently has several widely used laboratory tests to more rapidly assess the ASR risk of aggregates and durability of concrete mixtures. ASTM C1260 uses an extremely accelerated testing environment (specimens are stored in 1N NaOH at 80^{O}C) to reduce the testing time to 16 days, but this dramatically reduces the test reliability. ASTM C1293 uses less harsh conditions (100% relative humidity at 38^{o}C) to accelerate the reaction to identify reactive aggregates in 1 year, but an experimental artifact called alkali leaching can ultimately stop ASR, leading to possible false aggregate identification.

The motivation, objectives, and outline of this thesis are described in Chapter 1. Chapter 2 details the development and evaluation of two new tests to identify ASR. These new tests address the flaws in existing ASTM testing methods. In the sealed concrete prism test (S-CPT), a membrane is applied to the surface of concrete prisms to prevent alkali leaching. In the water entrained concrete prism tests (WE-CPT) the same moisture barrier prevents alkali leaching, but pre-saturated light weight aggregates are added to the mixture to provide excess moisture for expanding ASR gel. Four varying levels of reactive aggregates were tested at both 38^{o}C and 60^{o}C, to determine the effectiveness of these new test methods and the possibility of accelerating the tests. Expansion, mass change, relative humidity, and pore solution chemistry were experimentally measured to evaluate S-CPT and WE-CPT. The results suggest that alkali leaching can be lessened by a moisture barrier and important relationships between expansion, mass gain, and relative humidity were developed during this research.

In Appendix A, various moisture barriers were tested for their effectiveness at creating the closed system necessary for S-CPT and WE-CPT. Based on the results, a vapor permeable membrane was selected and used in S-CPT and WE-CPT because it was able to lessen alkali and OH^{-} leaching, while also maintaining ASR promoting levels of relative humidity inside concrete. Subsequent Appendices present experimental results for ASR tests conducted during this research.

TABLE OF CONTENTS

LIST OF FIGURES

LIST OF TABLES

ACKNOWLEDGEMENTS

Foremost, I would like to thank the support and guidance from my advisor, Dr. Rajabipour. The valuable assistance, comments, and advice he provided greatly influenced my learning during my graduate studies. I would also like to thank my thesis committee, Dr. Memari and Dr. Burgos for their useful suggestion and comments that shaped my research. I would also like to thank my fellow researchers and friends at CITEL for their support and companionship.

I would like to thank the financial support provided by the National Science Foundation. Without their assistance this research project could not have been completed. Any opinions, findings and conclusions or recommendations expressed in this thesis are those of the author and do not necessarily reflect the views of the National Science Foundation.

Lastly, I would also like to thank my Mom, Dad, and family for their never-ending love and support.

Chapter 1

Introduction and Thesis Outline

Motivation

Alkali-silica reaction (ASR) is a leading cause of premature concrete deterioration, leading to increased maintenance costs and a shortened service life for affected structures (including highway pavements and bridges, walls, dams, and roadway barriers). ASR occurs when metastable forms of silica in aggregates dissolve in the highly alkaline pore solution of concrete, and then form an expansive silicate gel that swells in the presence of moisture (Rajabipour et al. 2015). ASR results in cracks that create pathways for other forms of deterioration (freeze thaw damage, rebar corrosion, and chemical attack) to rapidly reduce the serviceability of the structure.

Many natural aggregates used in concrete mixtures are ASR prone, however the reaction typically takes 10 to 20 years to show symptoms. Therefore, accurate and quick laboratory test methods are needed to identify the potential for ASR. When aggregate reactivity is accurately determined, preventative measures such as chemical or mineral admixtures, can be implemented to prevent ASR from occurring. Currently, the concrete prism test (CPT, ASTM C 1293-08) and the accelerated mortar bar test (AMBT, ASTM 1260-14) are the common standard laboratory tests used to identify the potential for ASR in aggregates, but these tests have noted flaws. CPT takes 1 to 2 years, and an experimental artifact influences the results. AMBT exposes mortars to unrealistically harsh conditions resulting in poor test reliability (Ideker et al. 2012).

Researchers have identified these flaws in the current standards and have developed new ways to identify ASR prone aggregates. Researchers have tried developing adaptations of AMBT that allow the incorporation of coarse aggregates, and have shown good correlation between the new test and CPT results (Latifee and Rangaraju 2015). Other groups have increased the size of the specimens tested to limit alkali leaching, while others have wrapped the specimens in high pH cloths (Yamada et al. 2014). While these tests have identified ASR, they provide external

sources of alkalis and expose concrete to unrealistic conditions. A paradigm shift is needed that removes external sources of alkalis, and instead creates a closed system that will better replicate field conditions.

Objectives

In this research two new ASR test methods were developed and evaluated; a sealed concrete prism test (S-CPT) and a water entrained concrete prism test (WE-CPT). Both tests attempt to create a closed system by sealing specimens using a breathable membrane to reduce alkali and OH^- leaching, while also maintaining high internal relative humidity necessary for ASR. In addition to sealing, WE-CPT entrains excess water into the concrete prisms through pre-wetted lightweight aggregates, which over time desorb water to the expanding ASR gel. These modifications allow field conditions to be more closely replicated (thereby improving test reliability), and also allow testing at higher temperatures, which increases the rate of ASR and decreases the necessary time of testing.

The main objectives of this research are:

(1) To limit alkali leaching from concrete prisms undergoing ASR testing, to improve reliability of the test results;

(2) To allow for the reduction of testing time by increasing temperature;

(3) To evaluate the applicability of these two novel tests using aggregates of various reactivities (from moderately to very highly reactive) in mixtures with or without ASR mitigation.

(4) To provide a better understanding of the relationships among ASR expansion, concrete moisture gain, internal relative humidity (RH), pore solution chemistry, and temperature.

Thesis Outline

The following chapter in this thesis is composed of a journal paper detailing the methodology, results, and conclusions of evaluating S-CPT and WE-CPT as new ASR performance tests. The Appendices include supporting information including the methodology and experimentation used to select the moisture barrier and the results from the ASR tests used during this study.

References

Rajabipour, F., Giannini, E., Dunant, C., Ideker, J. H., & Thomas, M. D. (2015). Alkali–silica reaction: Current understanding of the reaction mechanisms and the knowledge gaps. *Cement and Concrete Research*, *76*, 130-146.

Ideker, J. H., Bentivegna, A. F., Folliard, K. J., & Juenger, M. C. (2012). Do current laboratory test methods accurately predict alkali-silica reactivity?. *ACI Materials Journal*, *109*(4).

Latifee, E. and Rangaraju, P. (2015). "Miniature Concrete Prism Test: Rapid Test Method for Evaluating Alkali-Silica Reactivity of Aggregates." *J. Mater. Civ. Eng.*, 27(7), 04014215.

Yamada, K., Karasuda, S., Ogawa, S., Sagawa, Y., Osako, M., Hamada, H., & Isneini, M. (2014). CPT as an evaluation method of concrete mixture for ASR expansion. *Construction and Building Materials*, *64*, 184-191.

Chapter 2

Two New Performance Tests to Identify Alkali-Silica Reaction

Abstract

This paper details two new tests that were developed and evaluated to identify alkali-silica reaction (ASR), a leading cause of deterioration in concrete. Currently, there are two widely used ASTM standards to identify ASR. ASTM C1260-14 (accelerated mortar bar test) exposes mortar bars to harsh conditions to rapidly identify ASR, taking only 16 days to complete, but has poor reliability due to the extreme exposure conditions. ASTM C1293-08 (concrete prism test) uses a high humidity environment to provide accelerated conditions for ASR, but leads to an experimental artifact known as alkali leaching that can lead to false aggregate identification during the 1-year experiment. The new tests presented in this paper attempt to reduce alkali leaching by creating a closed system to better replicate filed concrete. With alkali leaching prevented in the sealed concrete prism test (S-CPT), the testing duration can be reduced to three months, by increasing the testing temperature to 60^{o}C. In addition to a moisture barrier, the water entrained concrete prism test (WE-CPT) entrains excess water through pre-saturated lightweight aggregates to provide extra water for ASR gel to imbibe. To test the effectiveness of S-CPT and WE-CPT, four aggregates with different reactivities were tested using ASTM C1293 mixture proportions. The expansion, mass gain, internal relative humidity, and pore solution chemistry were experimentally measured. The results show that the vapor permeable membrane lessens the extent of alkali leaching and maintains high internal relative humidity in concrete, but leads to lower expansions at both testing temperatures.

Background

ASR gel, which forms from the dissolution of silica supplied by reactive aggregates and the alkalis found in the pore solution of concrete, can imbibe water and swell (Stanton 1940). When the stresses developed by the gel exceed the tensile strength of the concrete microstructure,

cracking can occur. Cracks allow other forms of concrete deterioration, including freeze thaw damage, chemical attack, and rebar corrosion to occur faster, leading to a rapid decrease in serviceability of the concrete structure. Examples of ASR affected structures include highway pavements and bridges, dams, roadway barriers and nuclear power plants.

As ASR has continued to plague infrastructure, experimental techniques have been developed to identify ASR in susceptible aggregates and to evaluate the durability of concrete mixtures, and the effectiveness of ASR mitigation methods (e.g., use of supplementary cementitious materials or ASR inhibiting chemical admixtures). In this paper, the current laboratory techniques to determine the potential for ASR are discussed, highlighting the need for a new test. In addition, two new ASR performance tests addressing these needs were developed and evaluated.

Alkali-Silica Reaction Mechanisms

ASR gel is formed by a chemical reaction that occurs between amorphous or poorly crystalline siliceous material found in some aggregates and the alkali and hydroxyl ions in pore solution of concrete (Stanton 1940). The produced ASR gel can then imbibe water and expand, resulting in map cracks that characterize ASR deterioration. The reaction mechanisms have been widely researched and are described below.

When water and cement are mixed, the resulting pH of the pore solution is highly alkaline (typically pH>13). Hydroxyl ions (OH^-) attack the metastable silica that is found in many natural aggregates, leading to dissolved silica in the pore solution. Aggregates that have a highly crystalline structure are unlikely to undergo ASR since it is difficult for hydroxyl ions to break silica bonds, but hydroxyl groups can attack and degrade aggregates that have a more amorphous structure. Alkali ions (Na^+ and K^+) form alkali-silicate gels with the dissociated silica ions. Calcium ions can replace alkali ions in silica chains to form longer and denser alkali-silicate gels. In the presence of moisture, these gels can imbibe water and swell (Rajabipour et al. 2015). For ASR to occur and damage concrete, four reaction components are necessary:

- Metastable silica found in aggregates

- High pH pore solution to attack aggregates and sufficient alkalis to participate in forming alkali-silica gel
- A source of soluble calcium to allow gelation of silica and to buffer pH changes
- A source of moisture to cause swelling of ASR gel

Current ASTM ASR test methods

In actual field structures ASR can take years to manifest as cracks and deterioration. Even though field observations provide the most reliable indicator for ASR, the long observation time (minimum of 5 to 10 years) and specific details of the job mixture used (e.g., cement alkali content and w/cm) limit the practicality of using field observations for quantifying the potential for ASR in future concrete mixtures. Because of these limitations, rapid laboratory scale tests have been developed and critiqued (Thomas et al. 2006). ASTM has numerous standard methods including: chemical, petrographic, and length change methods to determine the potential for ASR in aggregates. The two most widely used and cited tests are ASTM C 1293-08b (concrete prism test, CPT) and ASTM C 1260-14 (accelerated mortar bar test, ABMT). The following sections describe these standards in detail and the pitfalls of each test.

AASHTO and other regulatory agencies have standard guidelines for proportioning concrete mixtures to mitigate ASR (using chemical or mineral admixtures) based on aggregate reactivity as determined by AMBT and CPT, the importance of the structure, and exposure conditions (AASHTO PP 65-10). Many previous research studies have investigated mineral and chemical admixtures that effectively mitigate ASR in new structures (Stark et al. 1993). Commonly, fly ash, slag, or lithium compounds are used to mitigate ASR, but other novel admixtures have also been investigated (Feng et al. 2005, Folliard et al. 2003, Malvar and Lenke 2006). Therefore, accurate test methods are necessary to quantify the potential for ASR in aggregates for correct prevention methods to be used.

Accelerated mortar bar test (ASTM C1260-14)

ASTM C 1260-14 (accelerated mortar bar test, AMBT) exposes 25.4 mm x 25.4 mm x 285 mm (1" x 1" x 11.25") mortar (cement, water, and sand) bars to an alkaline soak solution to exacerbate ASR (Figure 2-1). Aggregate gradation is specified to achieve a fineness modulus of 2.9; therefore coarse aggregates must be crushed to meet the size requirements. Mortar is mixed at a water to cement ratio of 0.47 (by mass) using 440 grams of cement and 990 grams of sand. Mortar bars are cast and after one day of curing at 23ºC in 100% relative humidity, followed by 24 hours storage inside a water bath stored at 80ºC the initial length of mortar bars is measured. Next, the bars are stored inside 1N NaOH bath at 80ºC, for 14 days, while subsequent comparator measurements are taken at two or three day intervals to determine the percent length change of mortar bars. After 14 days of exposure to the soak solution, expansions less than 0.1% are deemed innocuous, expansions greater than 0.2% are deleterious, and expansions falling between these ranges need further testing (ASTM C 1293-08).

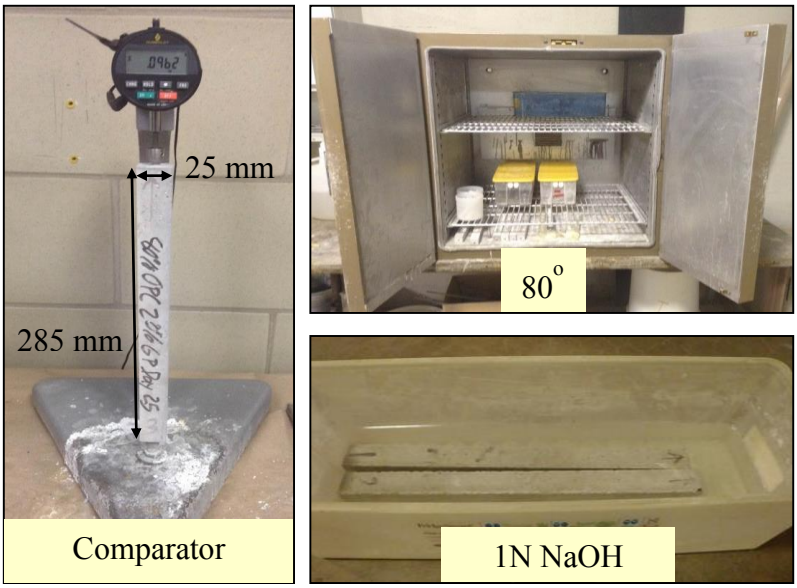

Figure **2-1**: Experimental setup for ASTM C1260. Mortar bars are stored in 1M NaOH at 80ºC and the expansion is measured using a comparator.

The accelerated mortar bar test can be completed in 16 days to screen aggregates, but the harsh exposure conditions adversely affect the test reliability. The harsh conditions lead to numerous false positives, false negatives and discrepancies between field performance and

AMBT. Numerous false positive results have been reported by Bérubé and Fournier; meaning an aggregate can fail AMBT, but shows no ASR in the field (Bérubé and Fournier 1993). Though less common, false negative results are more dangerous, resulting in an aggregate thought to be innocuous (using AMBT) showing deleterious ASR in the field (Bérubé and Fournier 1993, Hooton and Rogers 1992). Researchers have noted that AMBT should only be used to accept an aggregate as non-reactive, but further testing is needed to determine if an aggregate is reactive (Ideker et al. 2012).

Concrete prism test (ASTM C 1293-08b)

ASTM C 1293-08b creates a high humidity environment at a warm temperature (38ºC) to promote ASR gel formation in concrete prisms. The 75mm x 75 mm x 285 mm (3" x 3" x 11.25") prisms are stored in 25L airtight plastic buckets, over a small volume of water (20 mm), and lined with an absorptive felt to create a high humidity environment (Figure 2-2). CPT uses a high alkali Type I cement (0.9±0.1% Na_2O_{eq}) and the addition of NaOH to the mix water to provide excess alkalis (1.25% Na_2O_{eq}, 5.25 kg/m^3) to accelerate expansion. Mixture proportions are set according to the standard and unknown or reactive aggregates are tested in combination with non-reactive aggregates (i.e. non-reactive coarse aggregate is tested with an unknown or reactive fine aggregate). After 24 hours of moist curing, prisms are demolded and an initial length measurement is taken using a comparator and then prims are transferred to the storage conditions. The length of each prism is recorded throughout testing duration and the percent length change is reported. To negate the effects of thermal expansion, prisms are allowed to cool to room temperature before measurements are taken. A length change greater than 0.04% at the final measurement (1 year for aggregates, 2 years for concrete mixtures containing ASR mitigating mineral or chemical admixtures) signifies the potential for deleterious ASR (ASTM C1293-08b).

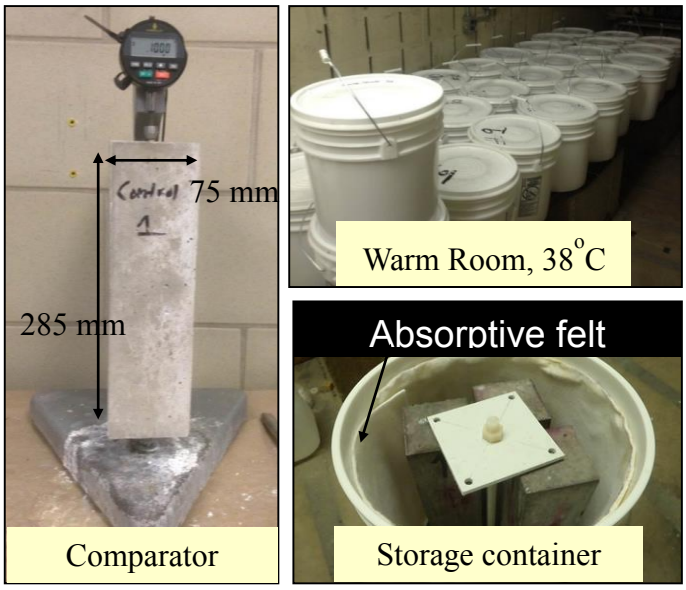

Figure **2-2**: Experimental setup for ASTM C1293. Concrete prisms are stored in 100% relative humidity at 38°C and the expansion is measured using a comparator.

Regarded as the most reliable ASR test method, CPT is used to quantify the potential for ASR in aggregates and concrete mixtures. CPT reports much fewer false positives than AMBT due to the less harsh conditions, but still reports the dangerous false negative results. Due to the high humidity environment and availability of water, some moisture condenses on the surface of the concrete prisms and draws the OH^- and alkali ions out of concrete pore solution, thus decreasing ASR (Figure 2-3). Alkali leaching affects the expansion of prisms, and can be seen as a plateauing of expansion over time (Figure 2-4) and was first reported by Blanks and Meissner (1946). Thomas et al. reported that 20% of the alkalis leach out of the prism in 90 days, and 35% leach out after 1 year of testing (Thomas et al. 2006). This significant decrease in alkali content can dramatically affect the expansion of prisms due to ASR, leading to false negative results. For construction projects that have a short project timeline, one year is also too long to wait for CPT to provide results on ASR. In short, while CPT is considered the most reliable existing ASR laboratory test method, it suffers from two significant drawbacks including: alkali leaching, which causes ASR to stop and a long test duration.

Figure **2-3**: Water condensed on the surface of the concrete prism. This water causes alkali leaching and ultimately stops ASR.

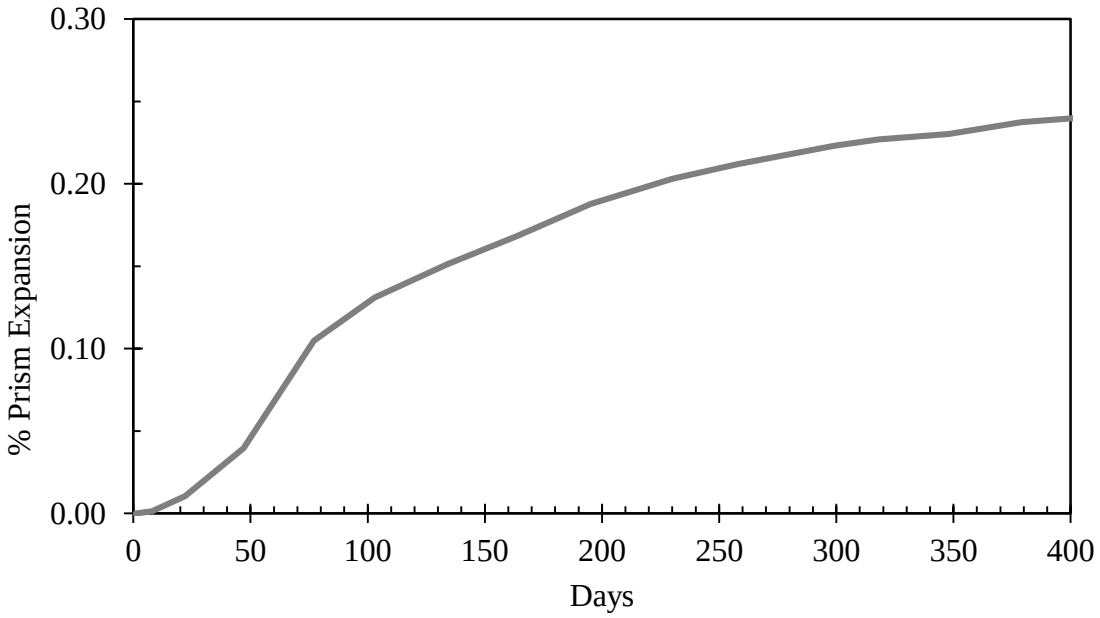

Figure **2-4**: Expansion plotted against time for a very reactive coarse aggregate. After approximately 150 days, the rate of expansion slows due to alkali leaching.

Other attempts at Novel ASR test methods

Since CPT became the common standard for identifying ASR, researchers have noted the long testing time, alkali leaching, and subsequent plateauing of expansion in CPT. Researchers have tried to decrease the testing duration by increasing the temperature, but have encountered an increased rate of alkali leaching (Folliard et al., 2004). Others have made modifications to the current standards (CPT and AMBT) to address the issues previously discussed. This section will detail previous attempts at novel ASR tests and the still present need for new tests.

Mini concrete prism test (M-CPT)

Research conducted by Latifee and Rangaraju modified AMBT to utilize both coarse and fine aggregates. By using 2"x"2"x11.25" concrete prisms, aggregates up to ½" in size could be tested eliminating the material alterations (i.e. crushing) necessary for AMBT. Similar to CPT, the cement used must have a high alkali content and additional alkalis are provided to reach a total of 1.25% Na_2O_{eq}. The mix proportions remain similar to CPT, noting only the volume fraction of coarse aggregate is reduced and the *w/c* is fixed at 0.45. The mixing and initial curing conditions also follow CPT, but after curing, prisms are demolded and placed inside water and stored at 60^{o}C for 24 hours. Initial length measurements are taken and the water is replaced with 1N NaOH soak solution similar to AMBT, but stored at 60^{o}C. Percent length change measurements are taken for 56 days, and expansions greater than 0.04% is considered indicative for potential ASR in field applications. The researchers reported agreement between MCPT and CPT test results (Latifee and Rangaraju, 2015).

While this test does address the issue of testing coarse and fine aggregates, it does not address the importance of alkali content and moisture availability and in short, does not replicate the field exposure conditions. By submerging concrete prisms in the NaOH soak solution; it exposes the prisms to an excess of alkalis and an unrealistically harsh environment. The soak solution provides an inexhaustible supply of alkalis to form ASR gel, unlike mass concrete, where the alkali content is fixed and can be exhausted/ consumed by ASR. Also a match between

MCPT and CPT is not necessarily indicative of a reliable test since CPT has its own reliability issues.

Accelerated concrete prism test (A-CPT)

A-CPT uses the same mixture proportions, mixing procedures, and curing conditions as CPT, but the storage temperature is increased from 38^{o} to 60^{o}C. The testing time is reduced from one year to 13 weeks. Ranc et al. (1992) were the first to investigate this idea, but other researchers have also investigated increasing the testing temperature of CPT and have noted that the test can be reproduced accurately (Ranc and Debray, 1992; Bolotte, 1992; Murdock and Blanchette 1994; Corneille and Bolotte, 1994; Touma et al. 2001; Folliard et al. 2004). The existing problem of alkali leaching is intensified at 60^{o}C, which can produce unreliable false negatives when testing low reactivity and slow reacting aggregates (Folliard et al. 2004). After 56 days of testing, the pH of the pore solution was measured and had dropped to 13.3, which leads to a significant plateauing of prisms and a lower overall expansion when compared to 38^{o}C (alkalis are leached out together with hydroxyl ions). Slow or moderately reactive aggregates could in-fact be deleterious in field structures, but due to alkali leaching, there is not enough alkalis for ASR gel to form during A-CPT (Ideker et al. 2006).

New ASR tests developed in this research

In this research project, two novel ASR performance tests were developed that address the flaws present in existing methods. A sealed concrete prism test (S-CPT) and a water-entrained concrete prism test (WE-CPT) were developed and evaluated for their applicability as ASR performance tests. A goal is to limit the rate of alkali leaching and this may allow the testing temperature to be increased to 60^{o}C to accelerate the test. Based on the work done by Thomas et al. in 2006, there is strong correlation between 13-week (3-month) expansion at 60^{o}C and standard CPT, which has also been shown to have strong correlation to field performance (Thomas et al. 2006).

Therefore, a 13-week expansion limit of 0.04% will be used to screen aggregates tested in this study.

Sealed concrete prism test (S-CPT)

To address the issue of alkali leaching from prisms undergoing CPT, a moisture barrier was applied to the surface of the prisms. It was believed that by creating a barrier between the high humidity environment and the concrete surface, water that condenses on the barriers surface would be unable to draw out the concrete pore solution, thus preventing alkali leaching.

Initially, prisms were cast and sealed using various methods and commercially available products including: rubber compounds, low permeability membranes, asphalt emulsion, epoxies, and pore structure modifiers (Figure 2-1). The experimental plan and findings of these preliminary experiments can be found in Appendix A. Based on the results, a vapor permeable membrane, Tyvek, was chosen and stored in a high humidity environment to prevent a loss of moisture. Vapor permeable membranes are able to prevent bulk water movements (liquid water), but allow water vapor diffusion. It was thought that a vapor permeable membrane would be able to maintain high levels of internal relative humidity, while also preventing alkali leaching.

Figure **2-5**: Various sealed concrete prism specimens sealed using various moisture barriers. Tyvek tape is used on the third prism from the left and was used in all S-CPT and WE-CPT testing.

Prisms using the S-CPT method are created using identical mixture proportions to traditional CPT testing (ASTM C1293-08b). The alkali content was increased from 0.91% from the cement to 1.25% Na_2O_{eq} using NaOH pellets to mimic CPT and the noted agreement between CPT and outdoor exposure blocks (Thomas et al. 2006). Once the moisture barrier was applied to the surface of the prisms, the prisms were transferred to CPT storage conditions. Buckets were stored at both 38ºC and 60ºC to determine the effectiveness of S-CPT to accelerate ASR and reduce the testing time to 13 weeks.

Water entrained concrete prism test (WE-CPT)

The water entrained concrete prism test (WE-CPT), uses the same moisture barrier as S-CPT, but entrains excess water inside the concrete to provide internal moisture for ASR gel expansion. Using the ideas and principals from internal curing, lightweight aggregates were presaturated before mixing. Once in the concrete, these lightweight aggregates can desorb water, which can be used for gel expansion (Pour-Ghaz et al. 2012). The Mackenzie-Bentz equation, which calculates the mass of LWA needed to entrain water for a certain degree of hydration, was modified to account for both excess water needed for full cement hydration and for ASR gel expansion (Bentz et al. 2005). An additional term (V_{ASR}) was added to the equation, which represents the volume of water needed to exhibit 0.12% volumetric expansion. Assuming that 1 gram of water gained by the prism represents 1 cm^3 of ASR expansion, the mass of LWA could be calculated using Equation 1.

$$M_{LWA} = \frac{V_{ASR} + V_{CS}}{S\phi_{LWA}}\rho_W = \frac{V_{ASR} + C_f CS\alpha_{max}}{S\phi_{LWA}}\rho_W$$

where: V_{ASR} (L/m^3 of concrete) is the volume of water entrained for ASR gel expansion, V_{CS} (L/m^3 of concrete) is the volume of water to compensate for chemical shrinkage, C_f (kg/m^3 of concrete) is the cement content, CS is the chemical shrinkage of cement (assumed to be a common OPC value of 0.064 L/kg of cement), α_{max} is the maximum degree of hydration

(assumed to be full hydration, 100% for w/c = 0.45), S is the degree of saturation of LWA (assumed to be 100% since LWA is saturated for a full 72 hours), Φ_{LWA} is the absorption capacity of LWA, and ρ_W is the density of water.

Since LWA replaces a volume of aggregate, the volume of reactive aggregate used in WE-CPT mixtures must be kept the same as CPT and S-CPT. When a reactive coarse aggregate is being tested, a portion of the non-reactive fine aggregate is replaced with LWA. Similarly, to test reactive fine aggregates a portion of the non-reactive coarse aggregate is replaced with LWA on a per volume basis.

Materials and methods

Four concrete mixtures (three 100% OPC mixtures, and one ASR mitigated mixture using class F fly ash) using reactive aggregates, were tested to evaluate the relationships between the expansion, mass gain, and pore solution chemistry for CPT, S-CPT, and WE-CPT. In addition, S-CPT mixtures were made with non-reactive aggregates to quantify the amount of alkali leaching present in CPT, S-CPT, and WE-CTPT at both testing temperatures. Since ASR is minimal in samples that use non-reactive aggregates, any decrease in alkali and OH^- concentration can directly be linked to leaching. Mixtures developed and tested in this study can be found in Table 2-1.

The reactive aggregates used in this study were very highly reactive Jobe Sand from El Paso, Texas, highly reactive Spratt coarse aggregate from Ontario Canada, and a locally supplied, moderately reactive river sand. The non-reactive and moderately reactive aggregates were supplied by New Enterprise Stone and Lime. The Ministry of Transportation in Ontario supplied the reactive limestone coarse aggregate. An expanded shale lightweight aggregate, supplied by Hydrocure, was used to entrain water into concrete prisms undergoing WE-CPT. Aggregate properties can be found in Table 2-2.

Table **2-1**: Concrete mixtures tested in this study to evaluate CPT, S-CPT, and WE-CPT.

Mixture ID	Aggregate	Agg. reactivity per AASHTO PP-65	Non-reactive aggregate	Binder	Is ASR mitigated?	CPT		S-CPT		WE-CPT	
						38C	60C	38C	60C	38C	60C
I	**Jobe (fine agg)**	Very highly reactive	Union Furnace (coarse agg)	100% OPC	No	✓	✓	✓	✓	✓	✓
II	**Spratt (coarse agg)**	Highly reactive	Oley (fine agg)	100% OPC	No	○		✓	✓	✓	✓
III	**Tyrone (fine agg)**	Moderately reactive	Union Furnace (coarse agg)	100% OPC	No	○	○	✓	✓	✓	✓
IV	**Tyrone (fine agg)**	Moderately reactive	Union Furnace (coarse agg)	75% OPC - 25% F fly ash	Yes	✓	✓	✓	✓	✓	✓
V	**Oley (fine agg)**	Non-reactive	Union Furnace (coarse agg)	100% OPC	No ASR	○		✓	✓		

○ = mixtures previously made at Penn State, ✓ = mixtures made during this research study

Table **2-2**: Aggregate properties for reactive, non-reactive, and light weight aggregates used in this study.

Aggregate	**Source location**	**Oven dry specific gravity**	**Dry rodded unit weight (kg/m^3)**	**Absorption (%)**	**AMBT 14-day expansion (%)**
		ASTM C127	ASTM C29	ASTM C127	ASTM C1260
Reactive Aggregates					
Jobe (fine agg)	Texas (USA)	2.58	N/A	0.96	0.68
Spratt (coarse agg)	Ottawa (Canada)	2.64	1,496.1	0.74	0.38
Tyrone (fine agg)	Pennsylvania (USA)	2.52	N/A	1.49	0.15
Non-reactive Aggregates					
Union Furnace (coarse agg)	Pennsylvania (USA)	2.7	1,475.3	0.44	0.075
Oley (fine agg)	Pennsylvania (USA)	2.7	N/A	0.46	0.076
Hydrocure LWA (fine agg)	Kentcky (USA)	1.40	N/A	22.3	0.049

Mixture proportioning and mixing procedures

The following mixture proportions were used to design and proportion the concrete mixtures described in Table 2-1. CPT and S-CPT use identical mixture proportions to ASTM C1293-08b. In CPT and S-CPT, the coarse aggregate content was set to 70% of the dry rodded unit weight (of the coarse aggregate) and the air content was assumed to be 2%. 420 kg/m^3 of cement was

used and mixed at a water to cement ratio (*w/c*) equal to 0.45. Reactive sand filled the remaining volume.

The modified Bentz equation was used to entrain extra water into the concrete mix for prisms undergoing WE-CPT. To keep the volume of reactive aggregate constant across all testing methods, the volume of non-reactive aggregate was decreased for WE-CPT (Table 2-3). The cement content and *w/c* ratio remained equal to CPT at 420kg/m^3 and 0.45 respectively. To allow for water absorption into LWA, the LWA was placed into the mix water (including NaOH used to reach 1.25% Na_2O_{eq}) for 72 hours. To limit the effects of carbonation, LWA that was being saturated with water was sealed in an airtight plastic bucket.

In all testing methods, the alkali content of the cement was boosted to 1.25% Na_2O_{eq}. The alkali content was artificially raised using NaOH pellets to replicate ASTM C1293. Materials were batched in the oven dry condition. Concrete mixing followed ASTM C 192 and was completed using an Enrich counter current mixer. Concrete samples were cast into 75mm x 75mm x 285 mm stainless steel molds with studs used for expansion measurements.

After 24 hours of curing at 100% RH chamber in 23^{o}C, prisms were demolded and surface of the prisms was allowed to air dry. The moisture barrier was applied to prisms undergoing S-CPT and WE-CPT testing, and initial mass measurements were recorded. The prisms were then transferred to the storage conditions described by ASTM C1293-08 and stored at 38^{o}C or 60^{o}C (Figure 2-6). After one day of storage to allow for thermal expansion, initial length measurements were recorded.

Figure **2-6**: Left: 60^{o}C oven and storage buckets used in this study. Center: 38^{o}C warm room and buckets used in this study. Right: Sealed prisms placed in identical storage conditions as described in ASTM C1293. These buckets were then stored at 38^{o}C or 60^{o}C.

Table **2-3**: Mixture proportions for CPT, S-CPT, and WE-CPT using the very highly reactive Jobe sand. Note: A portion of the non-reactive coarse aggregate was replaced by LWA in WE-CPT.

Mixture Proportions (kg/m^3 of concrete)			
	CPT	**S-CPT**	**WE-CPT**
Cement (kg/m^3)	420	420	420
Mix Water (kg/m^3)	199.21	199.21	223.98
Coarse Aggregate (kg/m^3)	1027.00	1027.00	837.00
Sand (kg/m^3)	702.22	702.22	702.22
LWA (kg/m^3)	-	-	119.32
Na_2Oeq (kg/m^3)	5.25	5.25	5.25

Cement and fly ash

The cement used in this study was a Lehigh Type I ordinary Portland cement, in accordance with ASTM C150, with an equivalent alkali content of 0.91% (ASTM C150-15). The cement oxide composition can be found in Table 2-4. The cement had 90.68% mass passing the No. 325 sieve (<45µm). The fly ash in this study was class F and the chemical and physical properties are found in Table 2-4.

Table **2-4**: Cement and fly ash properties used in mixtures created during this study.

Material Properties									
Portland Cement Oxide Composition								**Cement Physical Properties**	
SiO_2	Al_2O_3	Fe_2O_3	CaO	MgO	SO_3	Na_2O_{eq}	LOI	Density	Blaine Fineness (m^2/kg)
19.46	5.05	4.09	60.56	2.95	3.73	0.91	2.27	3.15	396
Fly Ash (class F) Oxide Composition								**Fly Ash Physical Properties**	
SiO_2	Al_2O_3	Fe_2O_3	CaO	MgO	SO_3	Na_2O	K_2O	LOI	Density	Fineness (retained on #325 sieve)
46.69	22.44	19.43	4.99	1.04	0.76	0.58	1.77	2.00	2.64	19.0%

Experimental Measurements

Expansion and mass change

To monitor and quantify the extent of ASR damage in concrete samples over time, the length change of the prisms was monitored using a digital comparator with an accuracy of 0.0001 millimeters. Due to the frequency of measurements, buckets were not cooled to room temperature before measurements were taken. Buckets were removed from the ovens and measured quickly in the same order (similar to AMBT procedures), to negate thermal effects. Initial measurements were taken 24 hours after prisms were transferred to buckets and stored at the testing temperature, to allow for initial thermal expansion and this length was recorded as the reference length of the prism. Subsequent expansion measurements were taken using the same methods.

After the length of each prism was recorded, excess moisture that has condensed on the sample were removed. Prisms were then weighed individually using an OHAUS digital balance with an accuracy of 0.1 grams. The initial mass (taken immediately after 24 hours of curing at 23^{o}C and 100%RH) was used as the reference.

Internal relative humidity (RH)

The internal relative humidity of prisms undergoing ASR testing was monitored to develop correlations between testing procedures and moisture avaliability. It has been previously suggested that ASR expansion occurs at relative humidities greater than 80 to 85% (Fournier et al. 2000). A commercially available concrete relative humidity kit (GE Protimeter) was used to measure the RH inside concrete. The bottom hole of the RH sleeve was removed to allow for RH measurements at a depth of 75mm (Figure 2-7). To prevent fresh paste from filling the sleeve, a metal rod was inserted into the sleeve during concrete placing and removed once the concrete was cured. After 24 hours of curing at 100% RH and 23^{o}C, the concrete prisms were demolded and the moisture barrier was applied to the surface of prisms undergoing S-CPT or WE-CPT testing. The plastic cap provide in the relative humidity kit was used to prevent moisture loss when the concrete prisms were not being measured. Concrete prisms were then transferred to identical stored conditions that were used to test CPT, S-CPT, and WE-CPT at 38^{o}C and 60^{o}C.

Internal RH measurements were taken using a GE Hygromaster digital RH meter, with an accuracy of 0.1%. Initial measurements were taken 7 days after casting to allow for initial equilibration between the concrete specimen and the plastic sleeve used for measurements. Before measurements, the plastic cap was removed from the plastic sleeve and a humidity sensor (GE Hygrostick) was inserted into the sleeve and measurements were taken using the RH meter. Measurements were recorded when the RH varied less than 0.1% for 15 minutes. Prior to measurements RH probes were tested for accuracy and calibrated by measuring known values of RH for saturated salt solutions.

Figure **2-7**: Experimental setup used to measure the relative humidity inside concrete specimens at a depth of 75 mm.

Pore solution analyses

Since limiting alkali leaching was paramount to developing new ASR tests, experiments were conducted to determine the effectiveness of the moisture barrier at preventing alkali leaching. Using pore solution extraction, the internal pore solution inside concrete could be obtained and subsequent titrations and ICP-AES analyses could determine the change in internal pH and alkali contents of the pore solution.

Figure **2-8**: Pore press setup showing: (A) crushed concrete with coarse aggregates removed, (B) assembled pore press device, and (C) pore press device under load. (Used with permission from Juliana Neves)

Periodically, sections of concrete prisms were removed from the storage conditions for pore fluid extractions (Figure 2-8). Samples were collected during the ASR initiation phase, maximum rate of expansion, and during the plateau of expansion. Samples were cooled to room temperature before pore solution extraction to prevent quick evaporation of the pore fluid. Once removed from the buckets, concrete sections were crushed into small pieces and large aggregates were removed as suggested by Cyr et al. (2008). Using a pore solution extraction device, the load was continually increased on the sample to 181,437 kg (400,000 lbs) at a rate of 18,148 kg/min (40,000 lbs/min). Between 0 and 5mL of pore solution was collected from each concrete sample and stored in a plastic vial. Immediately after extracting, pore fluid was filtered using a 0.2 µm-polypropylene filter and transferred to airtight vials with zero headspace.

Titrations were conducted to determine the pH of the pore solution. HCl solutions were made from 38.5% laboratory grade HCl and diluted using distilled de-ionized water to concentrations between 0.05 mol/L and 0.1 mol/L. 0.25mL of pore solution was diluted with de-ionized water and the color indicator phenolphthalein was added. Pore solution titrations were then conducted in triplicate to determine the OH^- concentration of concrete undergoing ASR. After titrations, the remaining pore solution was stored in airtight plastic vials with zero headspace, in a refrigerator until they were taken for ICP-AES analysis. ICP-AES analysis was conducted by laboratory staff at Penn State University using a Perkin-Elmer Optima 5300 UV ICP-AES to determine the elemental composition of the pore solution.

Results and Discussion

Expansion

The expansion for the concrete prisms containing the very highly reactive Jobe sand and tested in CPT, S-CPT, and WE-CPT are presented in Figure 2-9 (expansion curves for other aggregates can be found in Appendix B). For all aggregates tested, it can be seen that prisms stored at 60^{o}C expand more rapidly than the prisms stored at 38^{o}C. For the concrete prisms containing the very highly reactive Jobe sand, it takes less than one week to pass the expansion threshold of 0.04% at 60^{o}C, while the concrete prisms that are stored at 38^{o}C require an ASR incubation period before

the reaction begins. Unsealed concrete prisms, stored at 38ºC using the very highly reactive Jobe sand take 2 weeks to expand greater than the threshold, while it takes 4 weeks for the S-CPT and WE-CPT to surpass the threshold .

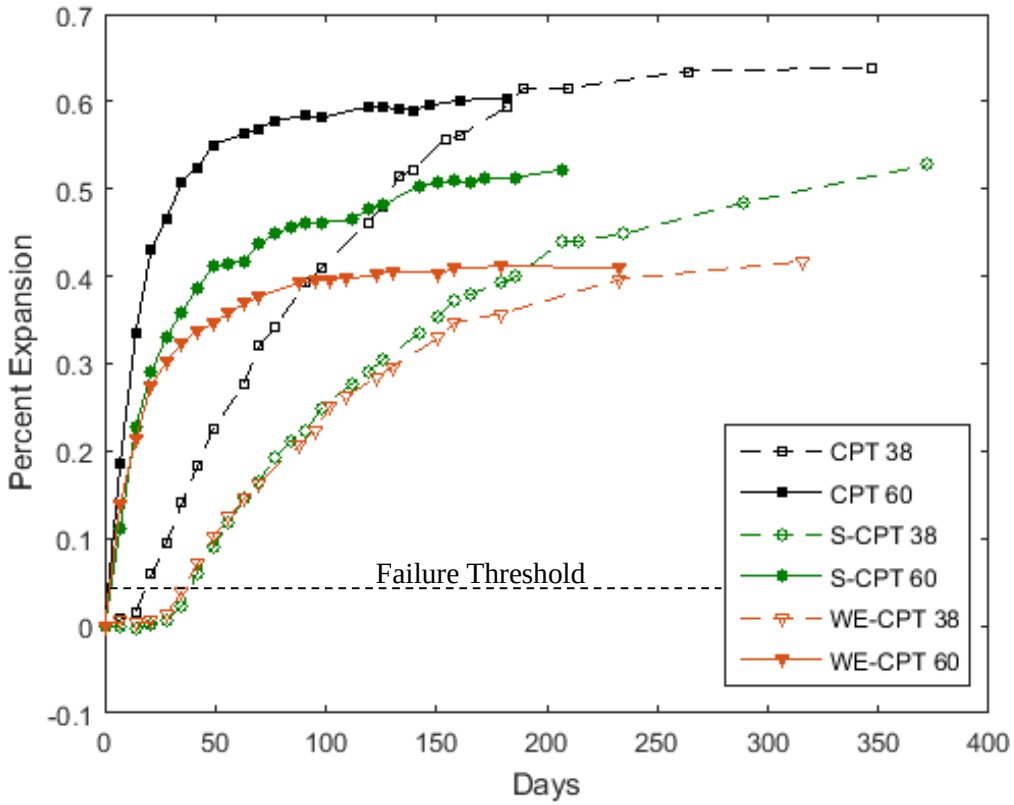

Figure **2-9**: Expansion of prisms undergoing ASR performance tests using very highly reactive Jobe fine aggregate.

In all tests, the prisms experience a plateauing of expansion. The plateau is more pronounced at 60ºC, and begins after 50 days of exposure. The prisms quickly expand before the plateau and high levels of expansion are measured, but the prisms maintain almost constant expansion after 50 days. At 38ºC, expansion continues to around 200 days, but then there is a decrease in the rate of expansion for all aggregates (including aggregates presented in Appendix B). Plateauing of expansion can be caused by a depletion of reactive silica, a depletion of hydroxyl and alkali ions, and a lack of available moisture. In these tests highly reactive aggregates are used, so it is unlikely that all sources of metastable silica have been consumed.

The high relative humidity inside the buckets also provides sufficient moisture for ASR gel to expand, so the plateauing of expansion is likely due to a decrease in hydroxyl and alkali ions.

In previous research where the testing temperature of CPT was raised to 60^{o}C, authors have noted expansion less than the expansion measured at 38^{o}C (Ideker et al. 2010). The decrease in expansion was attributed to an increased rate of alkali leaching and pH drop at the higher testing temperature. It is interesting to note that in this research all aggregates tested showed similar ultimate expansions at both 38^{o}C and 60^{o}C for each testing method.

It was thought that the addition of excess water through LWA particles would provide water to expanding ASR gel. There is only slight difference between S-CPT and WE-CPT at either 38^{o}C or 60^{o}C for specimens made with the highly reactive Jobe aggregate and this difference is smaller for the other three aggregates tested. The LWA particles are not aiding in the expansion, since they were determined to be unreactive during AMBT and they are also not acting as a sink for ASR gel expansion. SEM imaging was used to investigate whether ASR gel could be filling the voids of LWA, but no gel was found in the pore structure of many LWA particles that were imaged (Figure 2-10). Gel was found in the reactive Jobe aggregates and the ITZ between aggregates and the cement microstructure. The excess moisture that LWA particles were though to provide to expanding ASR gel, also had little impact on expansion. As the solution was desorbed, it would cause increased cement hydration which could densify the microstructure around the LWA particle. Densification would slow the ability for water to transport from the LWA particle to ASR gel.

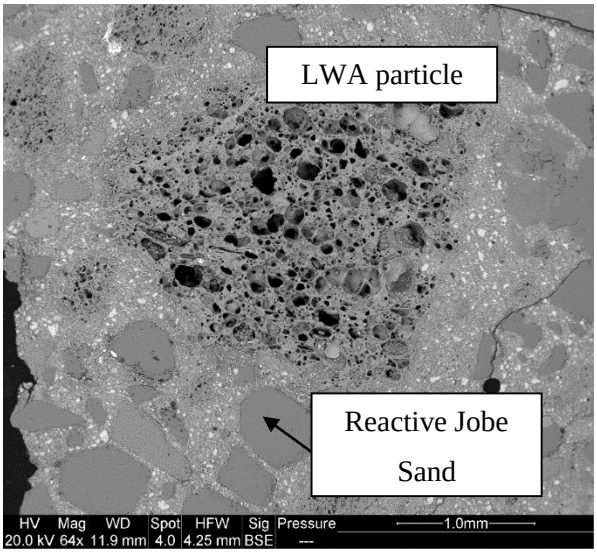

Figure **2-10**: LWA particle with no ASR gel filling the porous structure. Many locations were imaged and no ASR gel was found inside LWA voids.

Mass change

To prevent alkali leaching, a vapor permeable membrane was applied to the surface of concrete prisms to limit the ability for condensed water on the surface to draw out the ion from pore solution of concrete. To monitor the effectiveness of the barrier, the mass of each prism was measured and the percent mass change was calculated for the very highly reactive Jobe aggregates (Figure 2-11, and Appendix B for other aggregates).

When all aggregates tested are compared, the most expansive aggregates gain the most mass. For gel to become highly expansive, the prisms must uptake significant amounts of moisture. This is most evident for prisms stored at 60^{o}C, where unsealed CPT prisms uptake 1% of mass by 50 days (most expansive time). At 60^{o}C, once the plateau of expansion is reached, the prisms gain considerably less mass, possibly because new ASR gel is no longer being formed and the existing gel is not imbibing water.

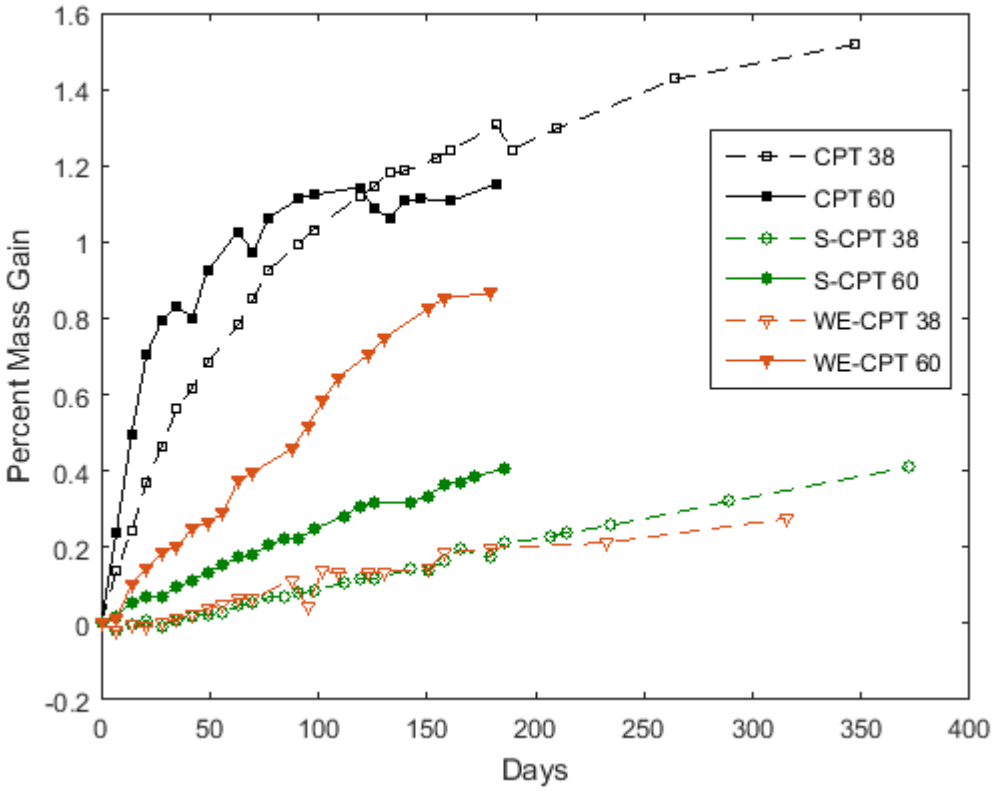

Figure **2-11**: Mass gain of prisms undergoing ASR performance tests using very highly reactive Jobe fine aggregate.

Unlike CPT, the sealed tests do not significantly gain mass during the most expansive period of ASR gel formation. The rate of mass gain is nearly linear for all sealed tests, since the rate of diffusion through the vapor permeable membrane governs the rate of moisture uptake. The slowed, but constant mass uptake reduces the availability of moisture for ASR gel expansion, which results in less and slower expansion, for all sealed tests and aggregates. At 60ºC, the rate of diffusion is increased, which explains the higher rate of mass uptake than prisms stored at 38ºC.

The presence of LWA particles also had an effect on the rate of mass gain. WE-CPT concrete prisms made using Jobe and Tyrone sand gain more mass than S-CPT specimens made with the same aggregate, when stored at 60ºC. As LWA particles desorb water, vapor remains in the aggregate's pores, and more moisture wants to fill these voids to maintain moisture equilibrium.

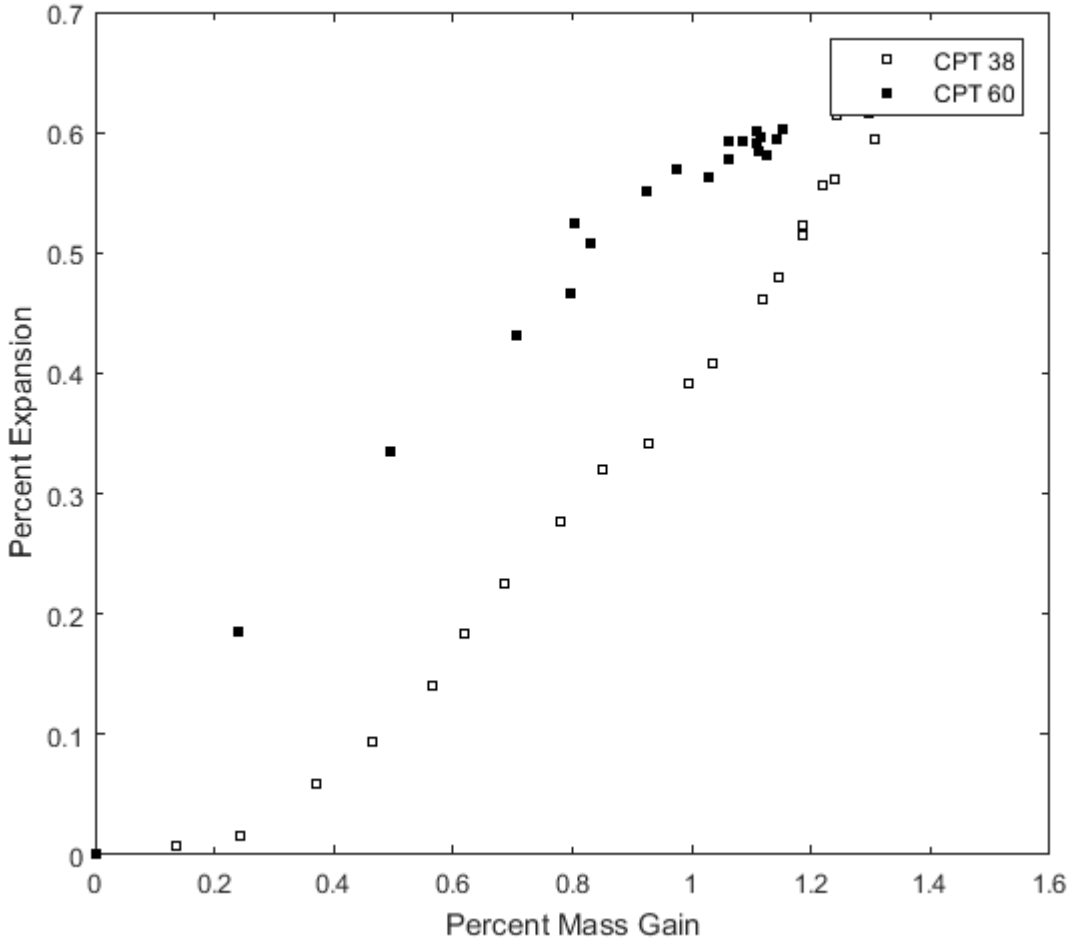

Figure **2-12**: Expansion vs. mass gain of unsealed prisms undergoing ASR performance tests using very highly reactive Jobe fine aggregate.

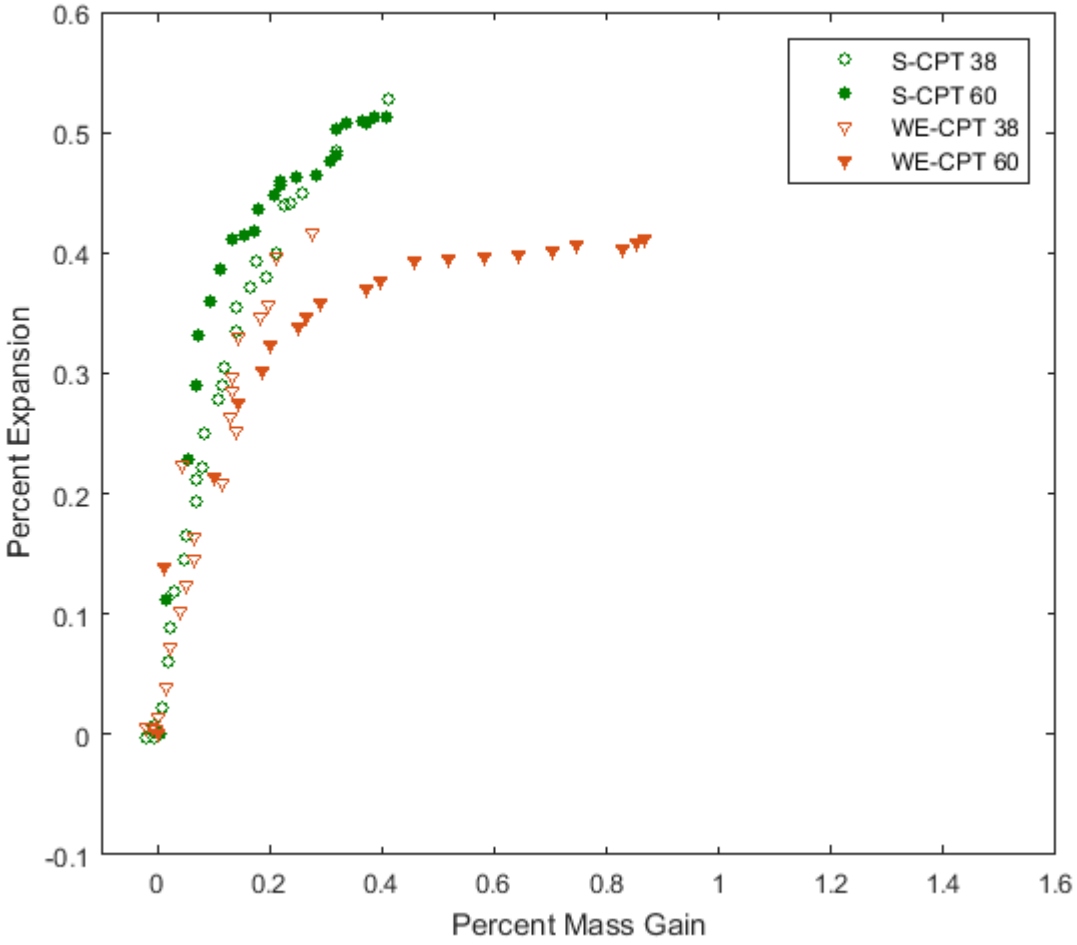

Figure **2-13**: Expansion vs. mass gain of sealed prisms undergoing ASR performance tests using very highly reactive Jobe fine aggregate.

When the percent expansion is plotted against the percent mass gain (Figure 2-12 and Figure 2-13), it can be seen that sealed prisms reach higher expansions at lower mass gain. There are fundamental differences between expansion and mass gain for sealed and unsealed tests. Sealed tests are more representative of the bulk concrete in service, which is why both sealed tests (S-CPT and WE-CPT) imbibe less water to reach equivalent levels of expansion.

Since there is no barrier that water must diffuse through, the mass gain in unsealed samples is higher. CPT prisms gain significant amounts of water during the initial few weeks of

testing, when the gel is expanding the most and the most water is being absorbed by concrete. The continued rate of mass gain is linear until ASR expansion and mass gain plateaus.

It is interesting to note that, all sealed tests have linear mass gain curves (Figure 2-13) before plateauing of expansion occurs. This is likely due to a decrease in alkali and hydroxyl concentrations that stops ASR, but water continues to diffuse through the membrane. Based on the results expansion is directly linked to the mass gain of the samples. Prisms that imbibe the most water expanded the most. This contradicts the assumption that 1 gram of mass gain directly correlated to 1mL of expansion, which was made in WE-CPT mixture proportioning.

Relative Humidity

The relative humidity inside concrete prisms was measured using a commercially available RH meter from GE (Figure 2-14). Various researchers have reported increased ASR expansions at higher humidity levels (Poyet et al. 2006). Relative humidites above 80% have been reported as the minimum for ASR gel expansion, while relative humidities ranging from 95-100% result in the maximum expansion (Olafasson 1992). In the new tests developed during this research, the relative humidites varied between 85-95%. The relative humidity was independent of the test methods, but was directly affected by testing temperature. At 38^{o}C, the relative humidity varied between 90-95%, while at 60^{o}C, the relative humidity varied between 85-90%. The vapor permeable membrane was able to maintain high relative humidities inside the concrete specimens, which promotes the formation and swelling of ASR gel. It is interesting to note that internal RH is not a good indicator of moisture uptake and mass gain of concrete prisms.

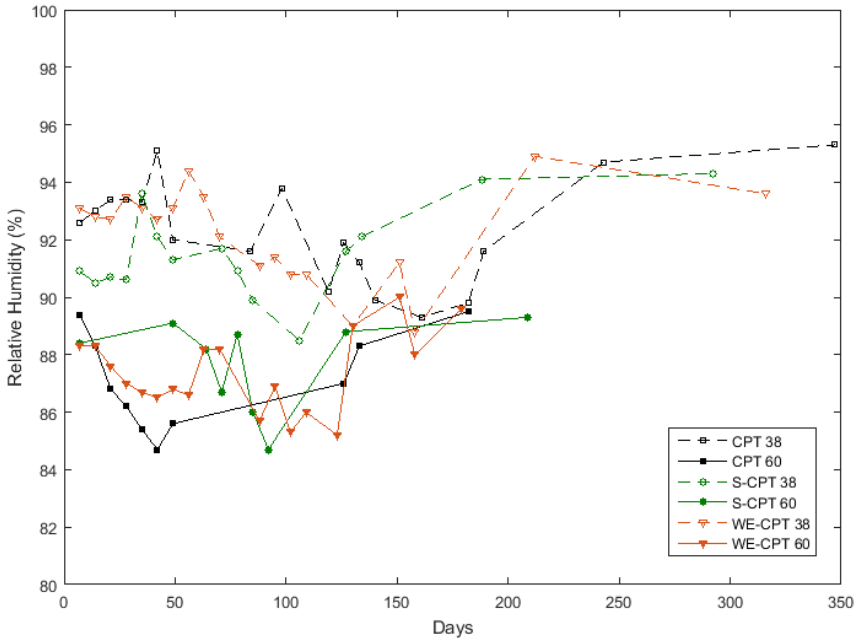

Figure **2-14**: Internal RH change during ASR testing for very highly reactive aggregate prisms stored at 38°C and 60°C. (Accuracy of GE Protimeter is ± 2%)

Alkali and OH^- Leaching

Reducing alkali and hydroxyl leaching was paramount to developing a more reliable ASR testing method. Pore solution from inside the concrete was obtained using a pore solution extraction device and the alkali and OH^- concentrations were analytically determined using titrations and ICP-AES. To quantify the amount of leaching, a non-reactive concrete mixture was cast and sealed using identical procedures as S-CPT. Since little ASR would be occurring in the specimens prepared with non-reactive aggregates, hydroxyl ions are not consumed during the reaction, and the associated decrease in pH can be directly contributed to leaching.

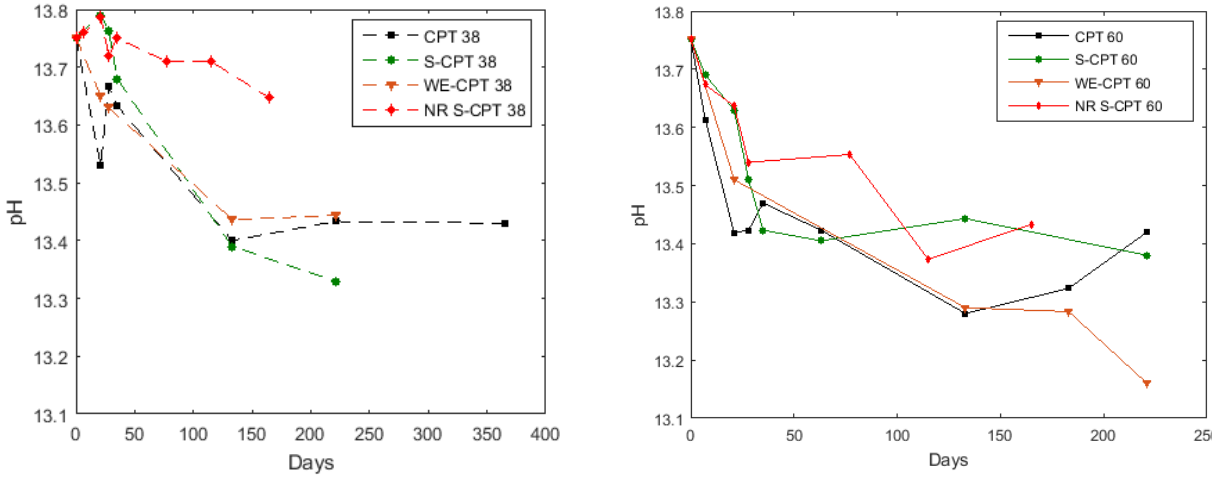

Figure **2-15**: Internal pH change during ASR testing for very highly reactive aggregate prisms stored at 38ºC and 60ºC. Average range of value is 0.019 pH units for each data point.

Initial pH and ion concentrations were collected 24 hours after moist curing, immediately before the specimens were sealed and transferred to the storage conditions. Subsequent measurements were taken during the ASR initiation phase, peak rate of expansion, and during the plateaued phase. At 38ºC, both S-CPT tests showed an increase in pH until 21 days. After 21 days, the pH in the S-CPT samples made with reactive Jobe sand decreased due to leaching and hydroxyl consumption during the degradation of aggregates. The decrease in pH in non-reactive (NR) samples is solely due to leaching (Figure 2-15).

At 60ºC, the decrease in hydroxyl concentration is more rapid because ASR occurs quicker at elevated temperatures. Between 0 and 50 days there is significant decrease in pH due to both consumption and leaching. S-CPT samples made with non-reactive aggregates experience decreasing pH, which can solely be due to leaching. Therefore, the moisture barrier is less effective at preventing alkali leaching at elevated temperatures.

Even though WE-CPT samples were sealed using the same membrane as S-CPT, the pH of the concrete pore solution in WE-CPT specimens decreased quicker at both testing temperatures. This is due to a dilution effect caused by the solution desorbed from LWA. The LWA was saturated with the mix water, including dissolved sodium hydroxide pellets to boost the alkali content in the mixture to 5.25 kg/m^3 (used to mimic ASTM C1293 mixture proportions). The resulting pH from the solution used to saturate LWA particles was 13.3, which

was lower than the pore solution of concrete. As this solution is desorbed from LWA it dilutes the pore solution, resulting in a lower pH than S-CPT.

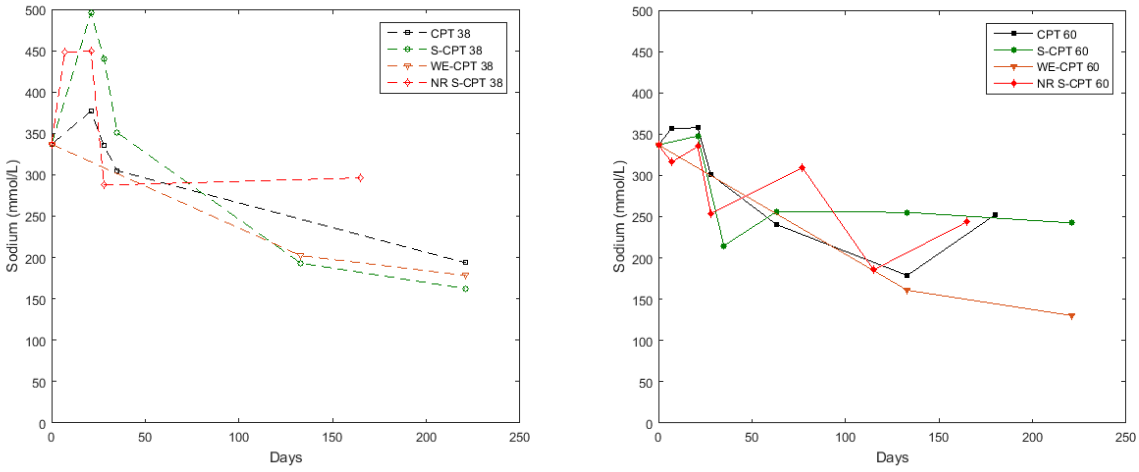

Figure **2-16**: Internal sodium concentration (mmol/L) change during ASR testing for very highly reactive aggregate prisms stored at 38°C and 60°C.

The sodium concentrations showed similar trends as the pH data for prisms undergoing ASR performance testing. At 38°C, there is an increase in sodium concentrations for both S-CPT tests up to 21 days, followed by a decrease in ion concentration (Figure 2-16). The moisture barrier is effective in decreasing sodium leaching at 38°C, since the non-reactive samples were able to maintain higher sodium concentrations throughout the test. At 60^0C, alkali leaching remains a persistent problem. Non-reactive specimens showed a decreasing trend in sodium concentrations and more closely followed the tests using the reactive aggregates.

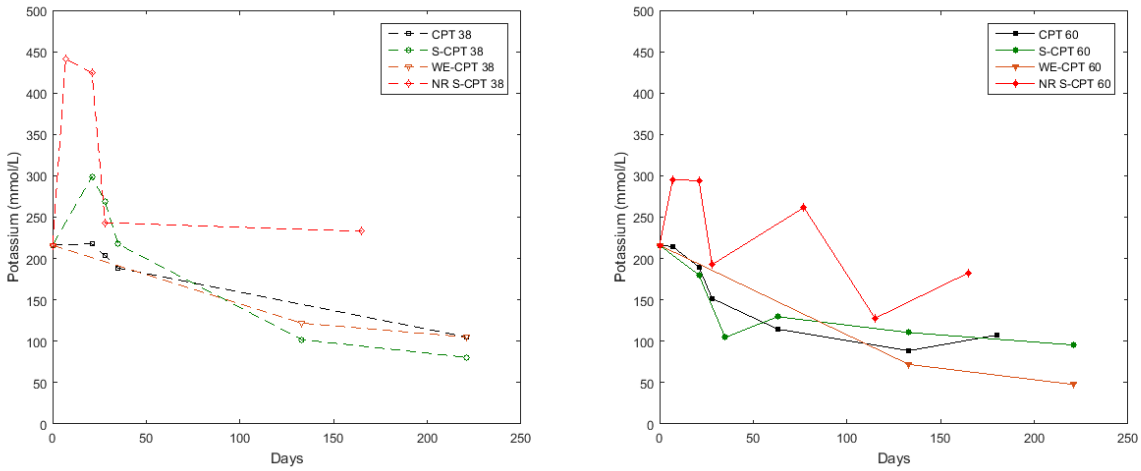

Figure **2-17**: Internal potassium concentration (mmol/L) change during ASR testing for very highly reactive aggregate prisms stored at 38ºC and 60ºC.

The decrease in potassium concentrations can directly be linked to both consumption and leaching during ASR testing (Figure 2-17). Both S-CPT tests again show an increase in concentrations up to 21 days, and then there is a decrease in concentrations as leaching and consumption occurs. The moisture barrier is effective in preventing some alkali leaching since the concentration, in specimens using non-reactive aggregates, remains constant from 35 days until 165 days. At 60ºC, the moisture barrier is able to maintain higher potassium concentrations in non-reactive specimens, but alkali leaching remains persistent due to increased diffusion.

When the testing temperature was increased to 60ºC, there was concern that sulfate concentrations would increase in the pore solution (Fournier et al. 2004). Sulfate would decrease the pH, therefore reducing the degradation of aggregates and ASR. Sulfur concentrations in the pore solution of prisms tested during this study did not show increased concentrations at the higher testing temperature (Figure 2-18). Therefore, the pH was not affected by an increase in sulfate concentrations.

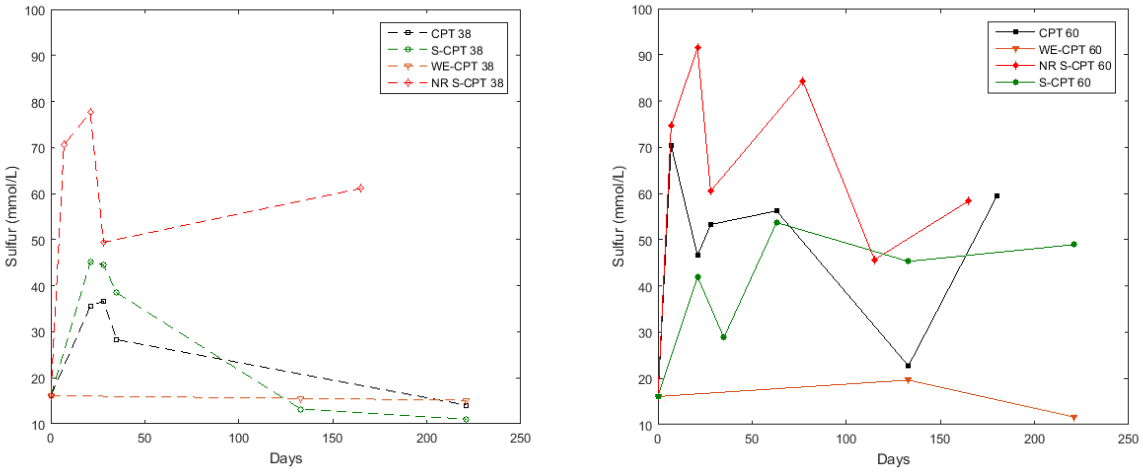

Figure **2-18**: Sulfur concentration (mmol/L) change during ASR testing for very highly reactive aggregate prisms stored at 38ºC and 60ºC.

Conclusions

The goal of this thesis was to investigate two new tests to identify alkali-silica reaction in concrete. Existing ASTM standards do not replicate filed conditions of concrete undergoing ASR. ASTM C1260, uses a highly alkali environment and high temperature to accelerate ASR, needing only 16 days to identify reactive aggregates. ASTM C1293, uses less harsh conditions, but is influenced by an artifact known as alkali leaching, which negatively impacts the reliability. The tests developed in this research, S-CPT and WE-CPT, attempted to create a closed system to more closely replicate field conditions of concrete. A moisture barrier was used to seal the concrete prisms and prevent leaching from the specimens. Five concrete mixtures were created using ASTM C1293 mixture proportions and tested using CPT, S-CPT, and WE-CPT at 38ºC and 60ºC. The expansion, mass gain, internal relative humidity, and changes in the pore solution chemistry were measured to determine the applicability of S-CPT and WE-CPT and to develop correlations between ASR expansion, mass gain, and pore solution chemistry. The main conclusions relating to the initial goals for this research are summarized below.

1. Limit alkali leaching from prisms:
    - Alkali and hydroxide leaching was lessened in tests that used a moisture barrier.
    - The vapor permeable membrane was ineffective at stopping alkali and hydroxyl leaching at 60^{o}C.

2. Decrease testing time:
    - Testing temperature was increased to 60^{o}C.
    - Equivalent expansions were reached at 60^{o}C in half the time
    - At 60^{o}C, plateauing occurs faster (due to leaching).

3. To evaluate the applicability of these two novel tests using aggregates of various reactivities (from moderately to very highly reactive) in mixtures with or without ASR mitigation:
    - Sealing prisms at 60^{o}C is ineffective at preventing leaching, but could be beneficial to preventing leaching at 38^{o}C.
    - The use of LWA in WE-CPT provides no benefits with the vapor permeable membrane tested in this study.

4. Provide correlations between ASR expansion, mass gain, internal relative humidity, and pore solution chemistry:
    - Unsealed prisms gain the most mass and expand the most.
    - The mass gain of prisms is directly related to the aggregate reactivity and the test method.
    - Internal relative humidities were 5% higher at 38^{o}C.
    - Plateauing of expansion is caused by the consumption and leaching of alkali and hydroxyl ions.

References

Stanton, T. E. (1942). Expansion of concrete through reaction between cement and aggregate. *Transactions of the American Society of Civil Engineers*, *107*(1), 54-84.

AASHTO PP 65-10. (2010). Standard Practice for Determining the Reactivity of Concrete Aggregates and Selecting Appropriate Measures for Preventing Deleterious Expansion in New Concrete Construction. American Association of State Highway and Transportation Officials, Washington, DC, 20 pp.

Rajabipour, F., Giannini, E., Dunant, C., Ideker, J. H., & Thomas, M. D. (2015). Alkali–silica reaction: Current understanding of the reaction mechanisms and the knowledge gaps. *Cement and Concrete Research*, *76*, 130-146.

Stark, D., Morgan, B., & Okamoto, P. (1993). Eliminating or minimizing alkali-silica reactivity. (No. SHRP-C-343).

Feng, X., Thomas, M. D. A., Bremner, T. W., Balcom, B. J., & Folliard, K. J. (2005). Studies on lithium salts to mitigate ASR-induced expansion in new concrete: a critical review. *Cement and Concrete Research*, *35*(9), 1789-1796.

Folliard, K. J., Thomas, M. D., & Kurtis, K. E. (2003). Guidelines for the use of lithium to mitigate or prevent ASR. (No. FHWA-RD-03-047).

Malvar, L. J., & Lenke, L. R. (2006). Efficiency of fly ash in mitigating alkali-silica reaction based on chemical composition. *ACI materials journal*, *103*(5)

Bleszynski, R., Hooton, R. D., Thomas, M. D., & Rogers, C. A. (2002). Durability of ternary blend concrete with silica fume and blast-furnace slag: laboratory and outdoor exposure site studies. *ACI Materials Journal*, *99*(5).

ASTM C1260-14. (2014). Standard Test Method for Potential Alkali Reactivity of Aggregates (Mortar-Bar Method). ASTM International, West Conshohocken, PA, www.astm.org

ASTM C1293-08b. (2008). Standard Test Method for Determination of Length Change of Concrete Due to Alkali-Silica Reaction, ASTM International, West Conshohocken, PA, www.astm.org

Blanks, R.F. and Meissner, H.S. (1946). The expansion test as a measure of alkali aggregate reaction. Journal of the American Concrete Institute, Vo. 17, No. 5, pp. 517- 539.

Thomas, M., Fournier, B., Folliard, K., Ideker, J., & Shehata, M. (2006). Test methods for evaluating preventive measures for controlling expansion due to alkali–silica reaction in concrete. *Cement and Concrete Research*, *36*(10), 1842-1856.

Latifee, E. R., & Rangaraju, P. R. (2014). Miniature Concrete Prism Test: Rapid Test Method for Evaluating Alkali-Silica Reactivity of Aggregates. Journal of Materials in Civil Engineering, 27(7), 04014215.

Ranc, R., & Debray, L. (1992). Reference test methods and a performance criterion for concrete structures. In *THE NINTH INTERNATIONAL CONFERENCE ON ALKALI-AGGREGATE REACTION IN CONCRETE, JULY 1992, LONDON, VOLUME 2*.

Bollotte, B. (1992). Development of an accelerated performance test on concrete for evaluating its resistance to AAR. In *9th International Conference on Alkali-Aggregate Reaction in Concrete, London, Conference Papers* (Vol. 1, pp. 110-116).

Murdock, K. J., & Blanchette, A. (1994). Rapid Evaluation of Alkali-Aggregate Reactivity Using a 60 C Concrete Prism Test. In *The 3rd International Conference on Durability of Concrete* (pp. 57-78).

Corneille, A. (1994). Results of a round robin test program for the validation of the test methods in the French recommendations for the prevention of AAR damage to concrete. *Special Publication*, *145*, 725-740.

Touma, W., Fowler, D., Carrasquillo, R., Folliard, K., & Nelson, N. (2001). Characterizing alkali-silica reactivity of aggregates using ASTM C 1293, ASTM C 1260, and their modifications. *Transportation Research Record: Journal of the Transportation Research Board*, (1757), 157-165.

Bérubé, M. A., & Fournier, B. (1993). Canadian experience with testing for alkali-aggregate reactivity in concrete. *Cement and Concrete Composites*,*15*(1), 27-47.

Folliard, K. J., Barborak, R., Drimalas, T., Du, L., Garber, S., Ideker, J. & Thomas, M. D. (2006). *Preventing ASR/DEF in new concrete: Final report*(No. FHWA/TX-06/0-4085-5)

Hooton, R. D., & Rogers, C. A. (1993). Development of the NBRI rapid mortar bar test leading to its use in North America. *Construction and Building Materials*, *7*(3), 145-148.

Ideker, J. H., Bentivegna, A. F., Folliard, K. J., & Juenger, M. C. (2012). Do current laboratory test methods accurately predict alkali-silica reactivity?.*ACI Materials Journal*, *109*(4).

Folliard, K. J., Ideker, J. A. S. O. N., Thomas, M. D., & Fournier, B. (2004). ASSESSING AGGREGATE REACTIVITY USING THE ACCELERATED CONCRETE PRISM TESTS. In *Aggregates: Asphalt Concrete, Portland Cement Concrete, Bases, and Fines. Twelfth Annual Symposium*.

Ideker, J., Folliard, K. J., Fournier, B., & Thomas, M. D. (2006). The Role of" Non-reactive" Aggregates in the Accelerated (60 C) Concrete Prism.

Pour-Ghaz, M., Castro, J., Kladivko, E. J., & Weiss, J. (2011). Characterizing lightweight aggregate desorption at high relative humidities using a pressure plate apparatus. *Journal of Materials in Civil Engineering*,*24*(8), 961-969.

Bentz, D. P., Lura, P., & Roberts, J. W. (2005). Mixture proportioning for internal curing. *Concrete International*, *27*(2), 35-40.

ASTM C150 / C150M-12. (2012). Standard Specification for Portland Cement, ASTM International, West Conshohocken, PA, ,www.astm.org

Fournier, B., Bérubé, M. A. (2000). Alkali-aggregate reaction in concrete: a review of basic concepts and engineering implications. *Canadian Journal of Civil Engineering*, *27*(2), 167-191.

Cyr, M., Rivard, P., Labrecque, F., & Daidie, A. (2008). High-Pressure Device for Fluid Extraction from Porous Materials: Application to Cement-Based Materials. *Journal of the American Ceramic Society*, *91*(8), 2653-2658.

Poyet, S., Sellier, A., Capra, B., Thèvenin-Foray, G., Torrenti, J. M., Tournier-Cognon, H., & Bourdarot, E. (2006). Influence of water on alkali-silica reaction: experimental study and numerical simulations. *Journal of Materials in civil Engineering*, *18*(4), 588-596.

Olafsson, H. (1992). Alkali-silica reaction—Icelandic experience. In *The Alkali Silica Reaction in Concrete* (pp. 208-222). Van Nostrand Reinhold New York.

Ideker, J. H., East, B. L., Folliard, K. J., Thomas, M. D., & Fournier, B. (2010). The current state of the accelerated concrete prism test. *Cement and Concrete Research*, *40*(4), 550-555.

Fournier, B., Chevrier, R., de Grosbois, M., Lisella, R., Folliard, K., Ideker, J., & Baxter, S. (2004, October). The accelerated concrete prism test (60 C): variability of the test method and proposed expansion limits. In *Proc. of the 12th Int. Conf. on AAR in Concrete, Beijing (China)* (pp. 314-323).

Appendix A

Finding a suitable moisture barrier

The novel tests developed in this research relied on a membrane to prevent alkali leaching from concrete specimens. Various barriers were investigated including: epoxy, paints, commercial concrete sealants, and commercially available membranes. To identify the effectiveness of barriers, various physical and chemical properties were experimentally measured and the results are described in Appendix A.

Vacuum Seal Bags - low humidity environment

Concrete prisms were cast using identical mixture proportions to ASTM C1293 and were sealed using a two-component barrier. Commercially available epoxies, water proofing paints, or asphalt compounds were applied directly to the concrete prisms and allowed to air dry for 24 hours (Table A-1 details the products that were tested). After drying, prisms were then placed in vacuum seal bags and the remaining air was removed from the bag by a pump. Samples were then placed and stored in bench top ovens at 60^{o}C.

Table **A-1**: Descriptions of the sealing methods applied to the surface of prisms before being placed in vacuum-sealed bags.

Product Name	Description
DryLOK	Masonry and concrete waterproofer
Hydro Halt	Paint on water and vapor barrier
Henry 107 Waterproofer	Asphalt Emulsion – sealer used for concrete and building products
Rustoleum concrete repair and patch epoxy	Two part, 100% solids epoxy
Prote Shield	Elastomeric Waterproof Sealer

To determine the effectiveness of the barriers at creating a closed system (i.e. no mass change) the mass of each sample was recorded using an OHAUS scale with an accuracy of 0.1 grams. Initial mass measurements were taken after the barriers had dried for 24 hours, but before prisms were placed in the vacuum seal-bags and the 60^{o}C oven. During subsequent

measurements, prisms were removed from the plastic vacuum bags before measurements were taken and were resealed in the bags before being returned to the ovens. The mass change for sealed prisms was monitored over a period of 30 days and the results of these experiments can be found in Figure A-1. Due to the low humidity environment inside the laboratory oven, moisture was drawn out of the specimens and mass loss for prisms was significant. These barriers and vacuum bags were not effective in creating a closed system. When prisms lose mass, the available water for ASR gel to imbibe decreases, negatively affecting the potential reliability of ASR testing methods. Therefore, more effective sealing methods had to be developed.

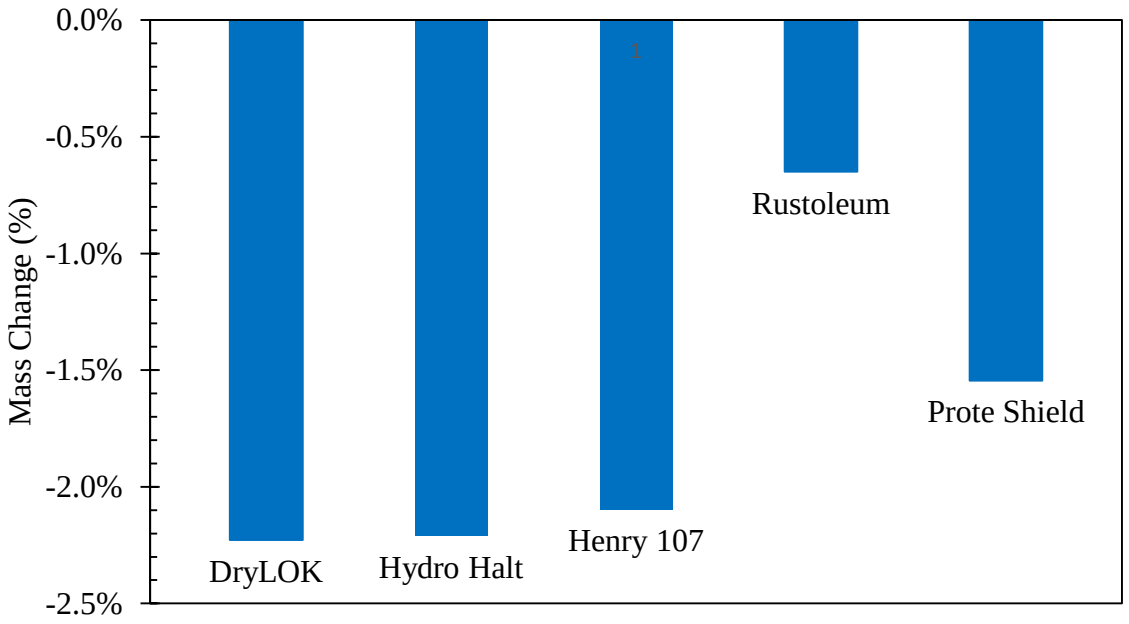

Figure **A-1**: Mass loss for prisms stored at 60ºC sealed using preliminary moisture barriers and vacuum-sealed bags. The mass loss was monitored for 30 days. No barrier was effective at creating a closed system.

Vacuum Seal Bags - high humidity environment

Since the initial barriers and vacuum seal bags that were tested lost mass in the low humidity environment, a high humidity (100% RH) environment was investigated. Sealed

concrete specimens (moisture barrier and vacuum seal bag) were placed on large plastic grates on plastic risers, above 25mm of water in large plastic tubs. A thin plastic film was placed on top of the plastic tub and then the lid was securely attached to prevent water loss from the storage environment. Similar to the bucket setup in ASTM C1293, this environment creates 100% relative humidity. Specimens were stored at 38^{o}C or 60^{o}C, to investigate the effectiveness of the barriers at elevated temperatures in high humidity environments.

Again, concrete prisms were cast using identical mixture proportions to ASTM C1293 and sealed using a two-barrier approach. Based on the performance of the barriers tested at low humidity environments, only Prote Shield or Rustoleum epoxy was applied to these prisms. A combination barrier was also investigated, that initially sealed the prisms using Prote Shield, followed by an application of Rustoleum Epoxy. After drying, sealed prisms were placed in vacuum bags and the remaining air was removed from the bag. Samples were then moved to the high humidity tubs in a warm room (38^{o}C) or bench top ovens at 60^{o}C.

The mass of the prisms was recorded using an OHAUS digital scale, with an accuracy of 0.1 grams. Initial mass measurements were taken 48 hours after demolding, since it took 24 hours for the Prote Shield to cure, and an additional 24 hours for the epoxy to cure. The mass of each prism was measured for 24 days and the percent mass change for the prisms was calculated (Figure A-2).

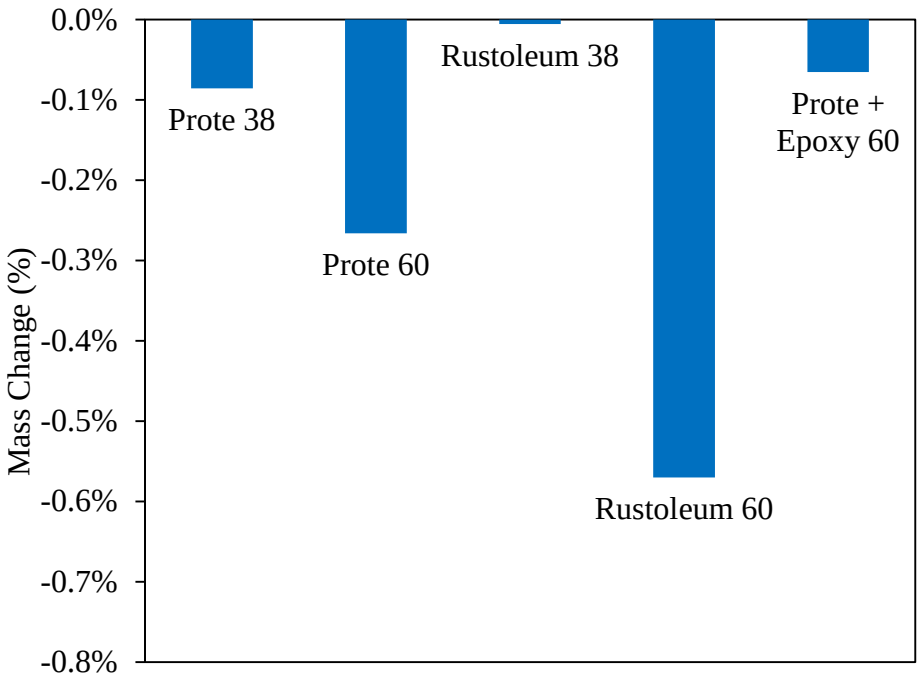

Figure **A-2**: Mass change for prisms stored in high humidity environments at 38°C and 60°C. Prisms were sealed using moisture barriers and vacuum-sealed bags. The percent mass change was monitored for 24 days.

It can be seen that placing the prisms in the high humidity environment improves the ability for the barriers to create a closed system. Even though the humidity in the environment was maintained at 100%, the prisms still lost mass through the barrier and plastic, which would limit the swelling capacity of ASR gel. Ultimately, due to the complex nature of the sealing process, persistent moisture loss, and the delicate nature of the plastic vacuum seal bags, new moisture barriers were tested.

Commercial Tapes

Due to the complexity and delicate nature of the vacuum-sealed specimens, simpler barriers were investigated. Due to importance of keeping moisture inside the specimen and preventing excess moisture from coming into the concrete prism, tapes with low moisture vapor

transmission rates (MVTR) were tested. Two tapes were selected based on low MVTR. An additional tape was selected that was vapor permeable, which allows air to pass through the membrane, but prevents bulk water movement. Both a single layer of tape and a double layer of tape were investigated. Tapes were applied to all surfaces of the prism with half of the tape overlapping the previous layer. For double wrapped prisms, the second layer of tape was applied in the opposite direction of the first layer.

Similar to the two previous experiments, concrete prisms were cast with identical size and mixture proportions to ASTM C1293, at a water to cement ratio of 0.45. Initial mass measurements were taken immediately after the tapes were applied and were recorded using an OHAUS scale with an accuracy of 0.1g. The mass of each sample was monitored during 3 weeks of testing and the percent mass change is presented in Figure A-3. After the prisms were sealed and weighed, they were transferred to identical storage conditions described in ASTM C1293-08b, but were stored at 60^{o}C.

The breathable membrane (Tyvek) provided the least mass change, and therefore created the most closed system. Since there wasn't a significant difference between double and single layers of tape, single layers of tape were used during future experiments. Based on visual observation, the aluminum tape was degrading in the high temperature and humidity environment, and could have been chemically reacting with concrete. Aluminum is a known mitigation strategy for ASR, therefore the direct contact between aluminum and concrete undergoing ASR testing is not desirable (Leemann et al. 2015).

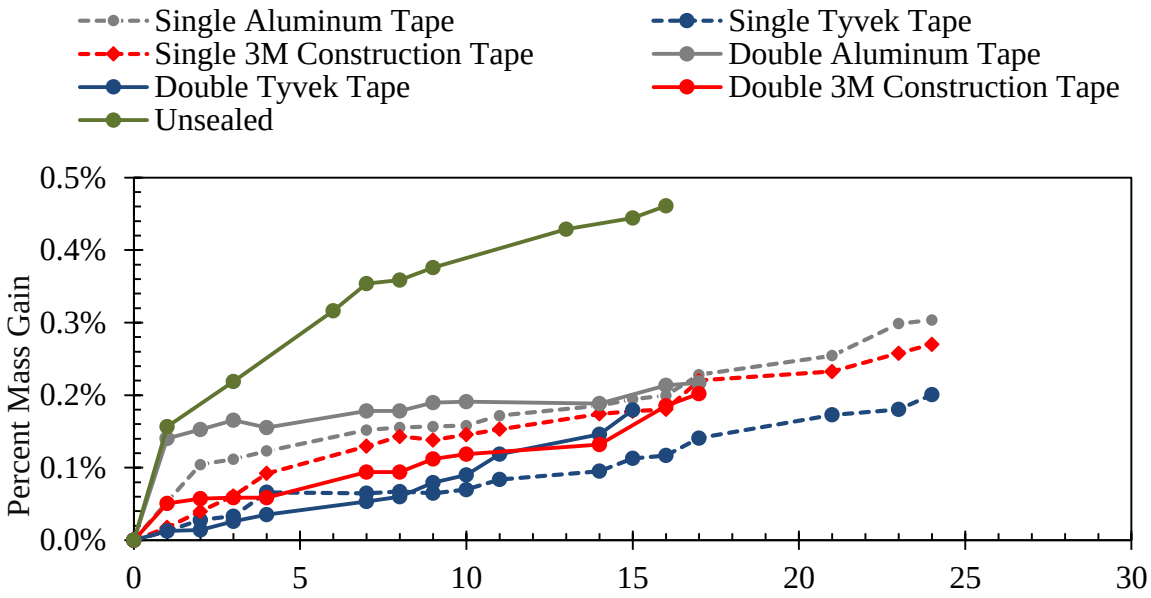

Figure **A-3**: Percent mass change for prisms wrapped in either a single or double layer of commercially available tapes. Prisms were stored in identical buckets and environments to ASTM C1293, but were kept at 60ºC.

Pore solution analysis of barrier systems

Additional tests were conducted to determine how the internal pore solution chemistry changed when concrete was sealed with various barriers, including the Tyvek. Samples were cast according to ASTM C1293-08b, but were cut into thirds along the lengthwise direction using a concert wet saw. The barriers were then applied to all sides of the 3" x 3" x 3 1/3" samples. Seven barriers were tested and are described in Table A-2. Aluminum tape was applied over a vapor permeable membrane to prevent direct contact between aluminum and concrete, due to the possibility of chemical reactions that would inhibit ASR.

Table **A-2**: Descriptions of the sealing methods applied to the surface of prisms before being placed in 100% RH in 38ºC or 60ºC.

Product Name	Description
Tyvek	Vapor permeable commercial home wrap
Tyvek + Aluminum	One layer of Tyvek, followed by one layer of aluminum tape
Perminator Tape	Very low moisture vapor transmission rate
Hydralastic 836	98% solids, liquid applied rubber compound
Mel-ROL	Cold applied asphalt membrane
Vapor-LOK	Liquid applied vapor proofer – creates more dense concrete microstructure

Immediately after sealing and initial mass measurement were recorded using an OHAUS digital balance with and accuracy of 0.1 grams. Prisms were transferred to high RH environments created by the buckets described in ASTM C-1293, at both 38ºC and 60ºC. Pore solution extraction was conducted at ages of 28, 56, and 100 days for prisms stored at 38ºC and 7, 28, and 56 days for prisms stored at 60ºC. Samples were also weighed at these times and the results are presented in Figure A-4. These ages were selected since they correspond to the initial start of ASR expansion, peak ASR expansion, and during the plateaued phase when expansion has slowed. These three ages provided critical insight into the evolution of pore solution chemistry during ASR for sealed and unsealed prisms.

Samples to be used for pore solution extraction were removed from the testing conditions at the predetermine ages and broken into small pieces. Coarse aggregates were removed before the crushed sample was loaded into the pore solution extraction device. Using a concrete compressive strength testing machine, the load was increased on the sample to 400,000 lbs, at a rate of 40,000 lbs/min. Pore solution was collected in a vial below the sample when under load. When pore solution was obtained from the concrete samples (note: some samples yielded no pore solution), the pore solution was immediately filtered using a 0.2 µm polypropylene filter and then 3 replicate titrations were conducted to determine the pH. The remaining pore solution was transferred to airtight plastic vials, with zero headspace, and stored in a 4ºC refrigerator until

ICP-AES was conducted to determine ion concentrations. Figure A-5 represents the change in pH for prisms stored at both testing temperatures.

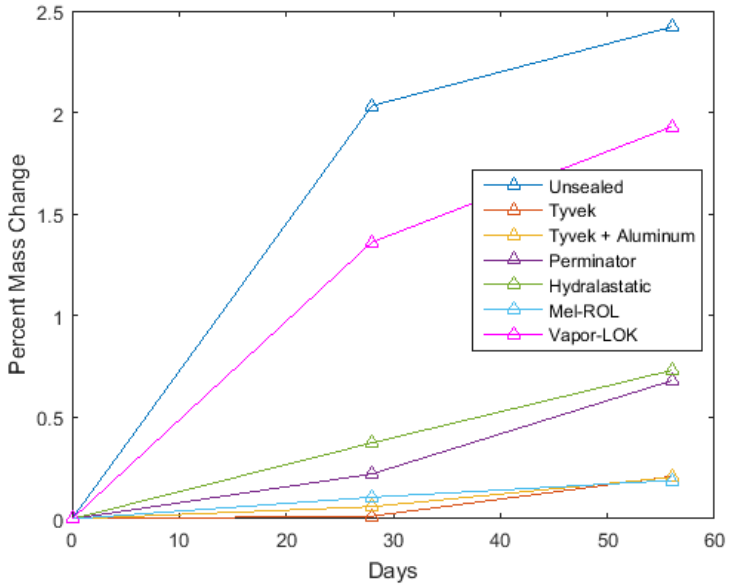

Figure **A-4**: Mass change for moisture barriers stored in 100% RH at 38ºC. Unsealed prisms gained the most mass, while the moisture barriers tested created a more ideal closed system.

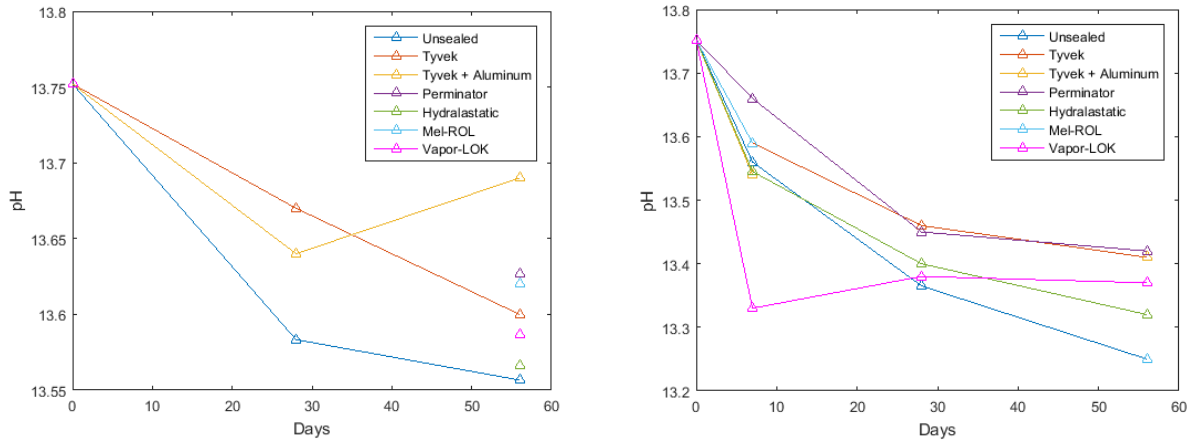

Figure A-5**:** Evolution of pH in concrete prisms undergoing ASR testing using moisture barriers. pH concentrations are expected to drop during testing due to consumption during ASR and by leaching.

Based on the mass gain results the membranes tested were able to create close to an ideal closed system. There was no significant difference between the mass change of permeable or impermeable membranes. The mass results for the membranes stored at 60^{o}C are not presented because some barriers melted or degraded and stuck to the storage bucket and accurate mass measurements were not possible. Barriers that showed visual signs of degradation were not used in future tests.

The pH and alkali content for all prisms decreased due to consumption by ASR since reactive aggregates were used in the concrete mixtures. Since all prisms were made from the same concrete mixture, any difference in OH^- and alkali concentrations can be attributed to a prevention of leaching. Unsealed prisms had the highest rate of alkali and OH^- leaching. Prisms that were sealed prevented some alkali leaching. At 60^{o}C, the tape applied (Tyvek, Tyvek + Aluminum, Perminator) had equal pH levels, showing that there is no difference in leaching prevention between vapor permeable or impermeable membranes. In future experiments a vapor permeable membrane (Tyvek) was used, since it provided a closed system that prevented significant mass gain and leaching.

Conclusions from moisture barrier experiments

Based on the experiments described and conducted in Appendix A, Tyvek was chosen as the moisture barrier to be used in S-CPT and WE-CPT testing. Tyvek was able to maintain high pH and alkali levels, while preventing significant mass change. Tyvek is also vapor permeable which will maintain the high relative humidities necessary for ASR inside concrete.

References

ASTM C1293-08b (2008), Standard Test Method for Determination of Length Change of Concrete Due to Alkali-Silica Reaction, ASTM International, West Conshohocken, PA, , www.astm.org

Leemann, A., Bernard, L., Alahrache, S. and Winnefeld, F., 2015. ASR prevention—Effect of aluminum and lithium ions on the reaction products.*Cement and Concrete Research*, *76*, pp.192-201.

Appendix B

Mixture proportions and results for other aggregate and concrete mixtures tested

Table **B-1**: Mixture proportions for CPT, S-CPT, and WE-CPT using the highly reactive Spratt coarse aggregate.

Mixture Proportions (kg/m^3 of concrete)			
	CPT	**S-CPT**	**WE-CPT**
Cement (kg/m^3)	420.0	420.0	420
Mix Water (kg/m^3)	200.0	200.0	223.7
Coarse Aggregate (kg/m^3)	1,047.3	1,047.3	1047.3
Sand (kg/m^3)	703.42	703.42	539.9
LWA (kg/m^3)	-	-	119.3
Na_2Oeq (kg/m^3)	5.25	5.25	5.25

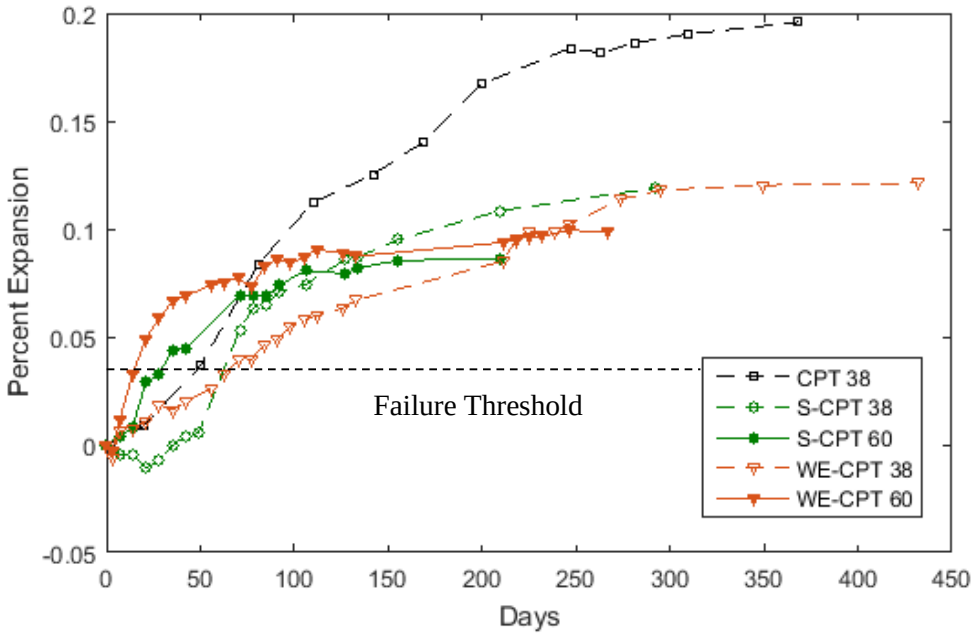

Figure **B-1**: Expansion of prisms undergoing ASR performance tests using highly reactive Spratt coarse aggregate.

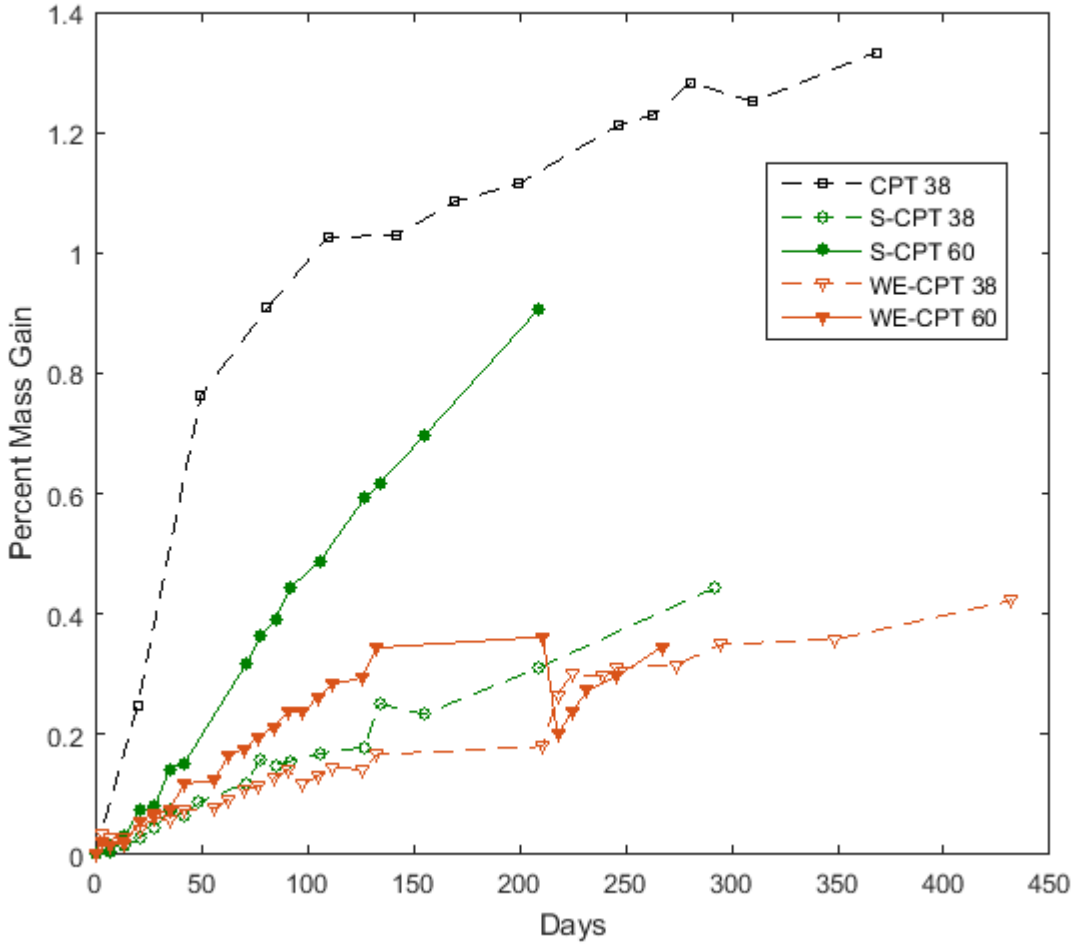

Figure **B-2**: Mass gain of prisms undergoing ASR performance tests using highly reactive Spratt coarse aggregate.

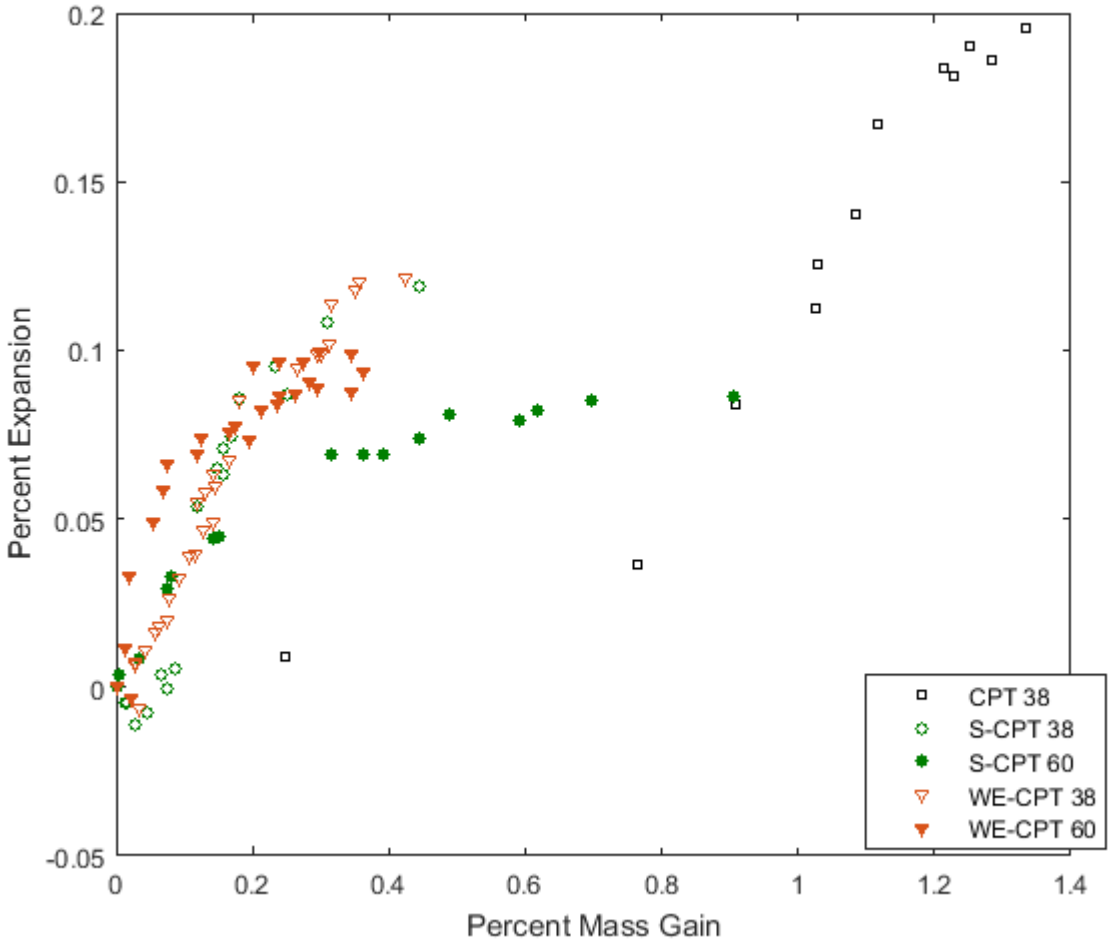

Figure **B-3**: Expansion vs. mass gain for prisms undergoing ASR performance tests using highly reactive Spratt coarse aggregate.

Table **B-2**: Mixture proportions for CPT, S-CPT, and WE-CPT using the moderately reactive Tyrone River Sand.

Mixture Proportions (kg/m^3 of concrete)			
	CPT	**S-CPT**	**WE-CPT**
Cement (kg/m^3)	420.0	420.0	420
Mix Water (kg/m^3)	203.9	203.9	228.0
Coarse Aggregate (kg/m^3)	1,032.7	1,032.7	837.0
Sand (kg/m^3)	692.3	692.3	692.3
LWA (kg/m^3)	-	-	119.3
Na_2Oeq (kg/m^3)	5.25	5.25	5.25

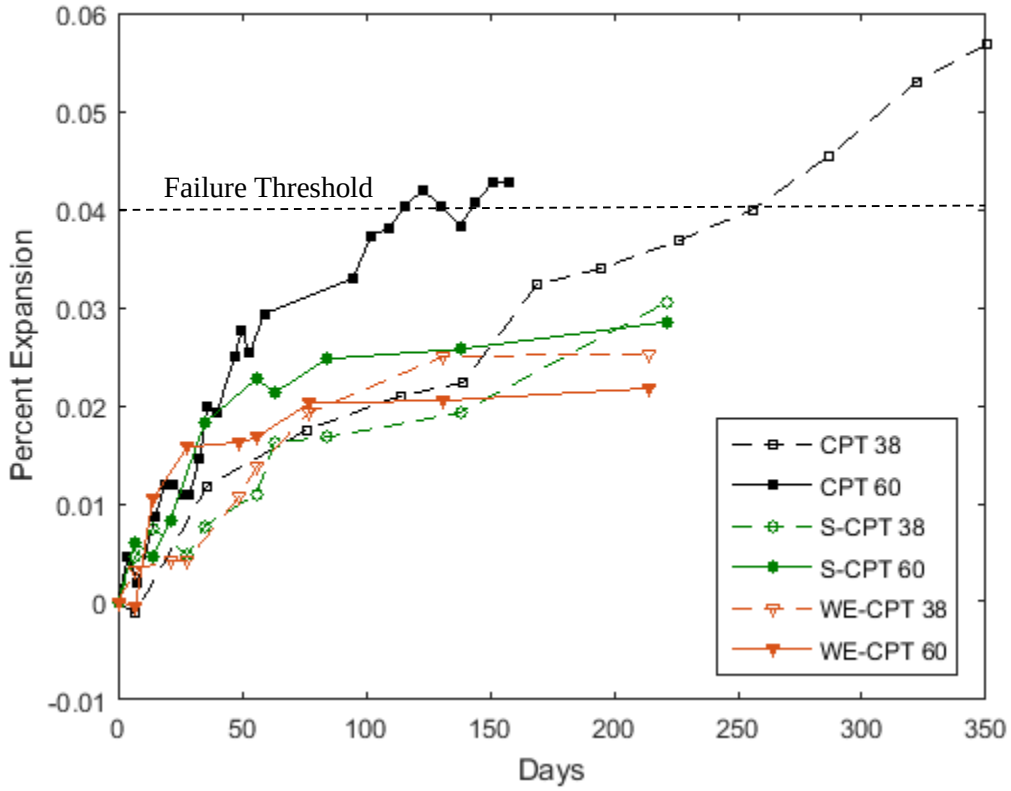

Figure **B-4**: Expansion of prisms undergoing ASR performance tests using moderately reactive Tyrone River Sand fine aggregate.

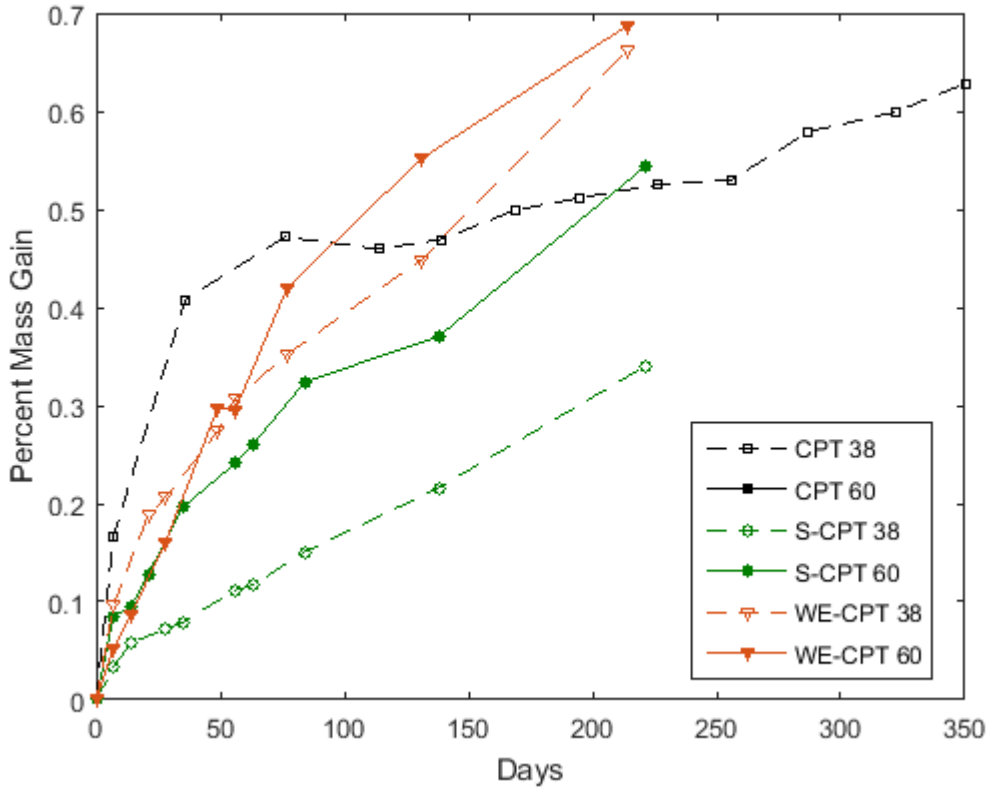

Figure **B-5**: Mass gain of prisms undergoing ASR performance tests using moderately reactive Tyrone River Sand fine aggregate.

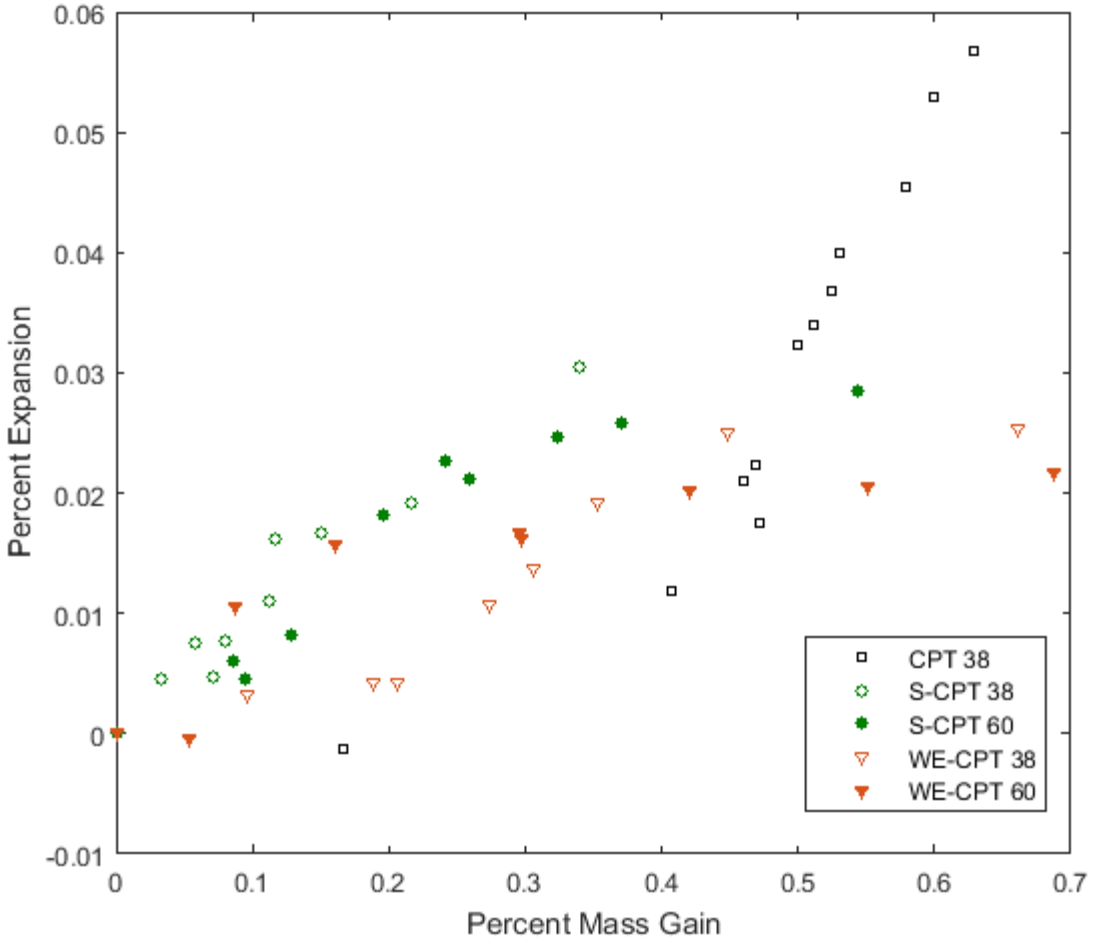

Figure **B-6**: Expansion vs. mass gain for prisms undergoing ASR performance tests using moderately reactive Tyrone River Sand fine aggregate.

Table **B-3**: Mixture proportions for CPT, S-CPT, and WE-CPT using Tyrone River sand and fly ash to mitigate ASR.

Mixture Proportions (kg/m^3 of concrete)			
	CPT	**S-CPT**	**WE-CPT**
Cement (kg/m^3)	315	315	315
Fly Ash (kg/m^3)	105	105	105
Mix Water (kg/m^3)	203.9	203.9	228.0
Coarse Aggregate (kg/m^3)	1,032.7	1,032.7	837.0
Sand (kg/m^3)	692.3	692.3	692.3
LWA (kg/m^3)	-	-	119.3
Na_2Oeq (kg/m^3)	5.25	5.25	5.25

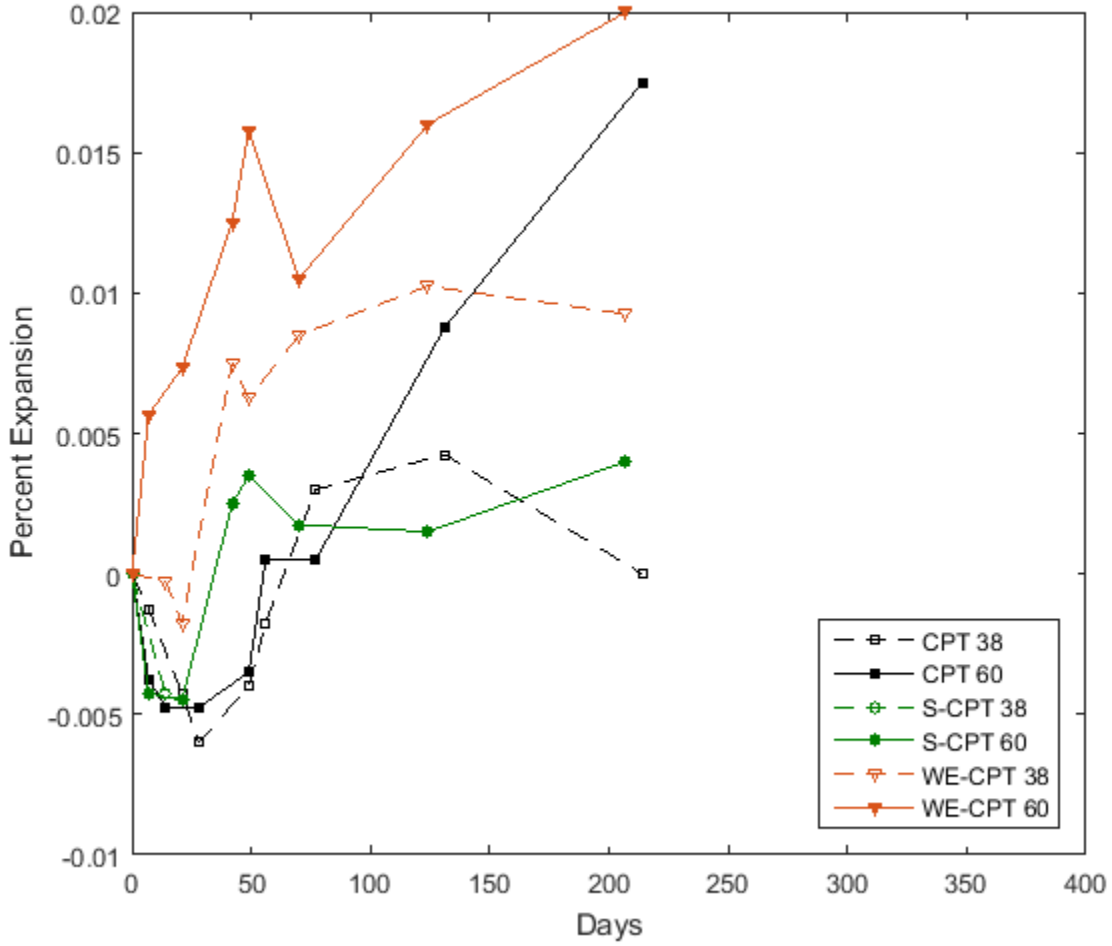

Figure **B-7**: Expansion of prisms undergoing ASR performance tests using moderately reactive Tyrone River Sand fine aggregate with 25% cement replacement with class F fly ash to mitigate ASR.

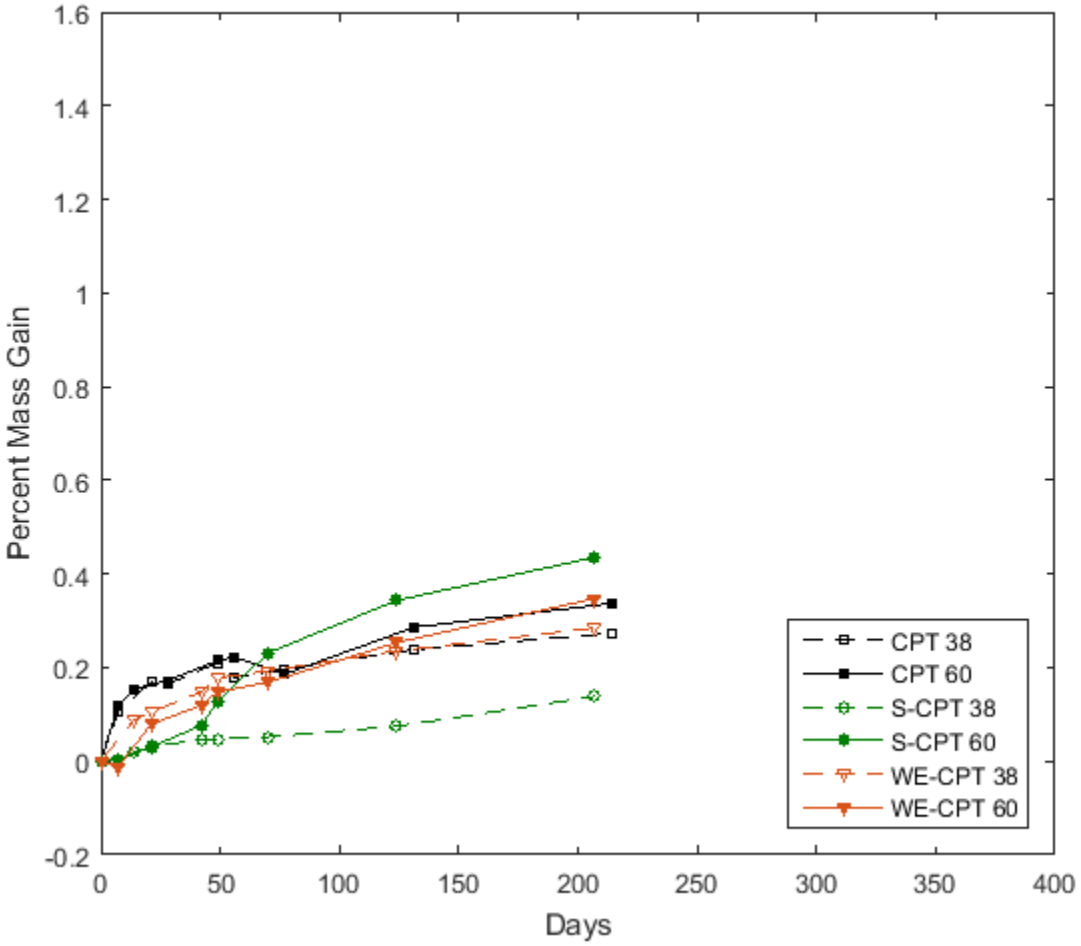

Figure **B-8**: Mass gain of prisms undergoing ASR performance tests using moderately reactive Tyrone River Sand fine aggregate with 25% cement replacement with class F fly ash to mitigate ASR.

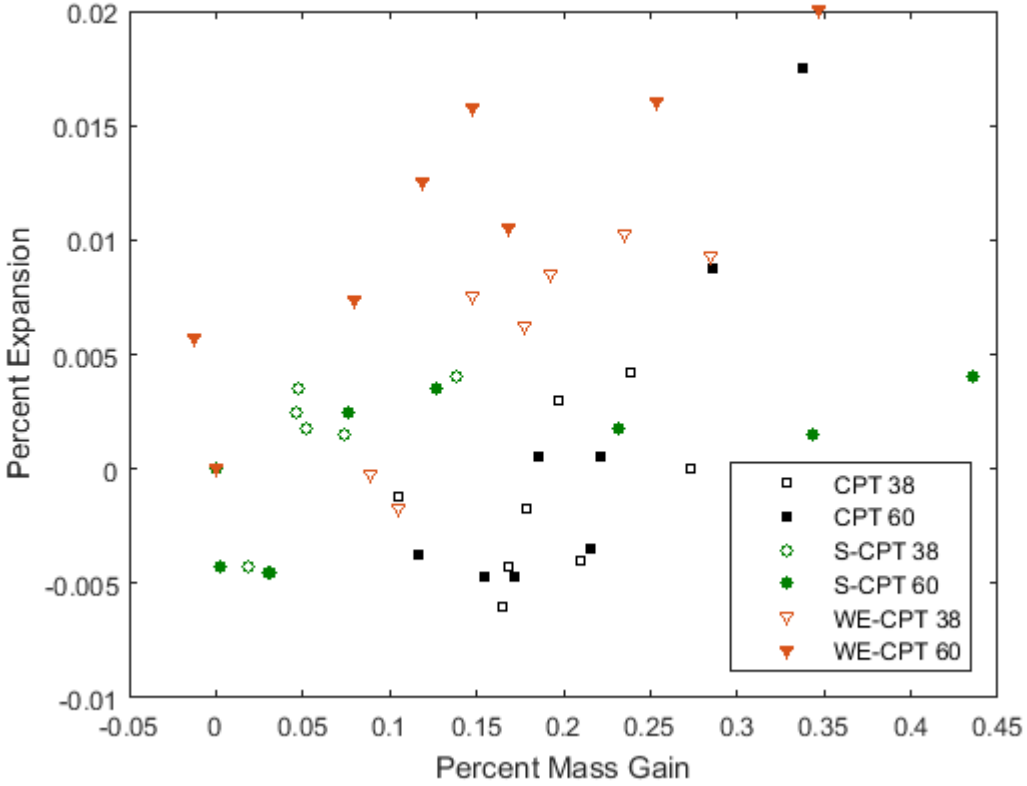

Figure **B-9**: Expansion vs. mass gain for prisms undergoing ASR performance tests using moderately reactive Tyrone River Sand fine aggregate with 25% cement replacement with class F fly ash to mitigate ASR.

Table **B-4**: Mixture proportions for S-CPT using two non-reactive aggregates.

Mixture Proportions (kg/m^3 of concrete)	
	S-CPT
Cement (kg/m^3)	420.0
Mix Water (kg/m^3)	200.0
Coarse Aggregate (kg/m^3)	1,032.7
Sand (kg/m^3)	741.8
LWA (kg/m^3)	-
Na_2Oeq (kg/m^3)	5.25

Appendix C

Compiled data for expansion, mass gain, and RH for concrete undergoing ASR testing

Table **C-1**: Expansion and mass gain results for CPT prisms made with very highly reactive Jobe aggregate.

CPT 38			**CPT 60**		
Day	Length (% Change)	Mass (% Change)	Day	Length (% Change)	Mass (% Change)
0	0.00	0.00	0	0.00	0.00
7	0.01	0.14	7	0.19	0.24
14	0.02	0.24	14	0.33	0.50
21	0.06	0.37	21	0.43	0.71
28	0.09	0.47	28	0.47	0.80
35	0.14	0.56	35	0.51	0.83
42	0.18	0.62	42	0.53	0.80
49	0.23	0.68	49	0.55	0.92
63	0.28	0.78	63	0.56	1.03
70	0.32	0.85	70	0.57	0.97
77	0.34	0.93	77	0.58	1.06
91	0.39	0.99	91	0.58	1.11
98	0.41	1.03	98	0.58	1.12
119	0.46	1.12	119	0.59	1.14
126	0.48	1.15	126	0.59	1.09
133	0.51	1.18	133	0.59	1.06
140	0.52	1.19	140	0.59	1.11
154	0.56	1.22	147	0.60	1.11
161	0.56	1.24	161	0.60	1.11
182	0.59	1.31	182	0.60	1.15
189	0.61	1.24			
210	0.62	1.30			
264	0.63	1.43			
347	0.64	1.52			

Table **C-2**: Expansion and mass gain results for S-CPT prisms made with very highly reactive Jobe aggregate.

S-CPT 38			S-CPT 60		
Day	Length (% Change)	Mass (% Change)	Day	Length (% Change)	Mass (% Change)
0	0.00	0.00	0	0.00	0.00
7	0.00	-0.02	7	0.11	0.02
14	0.00	0.00	14	0.23	0.06
21	0.00	0.01	21	0.29	0.07
28	0.01	-0.01	28	0.33	0.07
35	0.02	0.01	35	0.36	0.10
42	0.06	0.02	42	0.39	0.11
49	0.09	0.02	49	0.41	0.13
56	0.12	0.03	56	0.41	0.15
63	0.15	0.05	63	0.42	0.17
70	0.17	0.05	70	0.44	0.18
77	0.19	0.07	77	0.45	0.21
84	0.21	0.07	84	0.46	0.22
91	0.22	0.08	91	0.46	0.22
98	0.25	0.09	98	0.46	0.25
112	0.28	0.11	112	0.46	0.28
119	0.29	0.12	119	0.48	0.31
126	0.30	0.12	126	0.48	0.32
142	0.33	0.14	142	0.50	0.52
151	0.35	0.14	151	0.51	0.53
158	0.37	0.17	158	0.51	0.57
165	0.38	0.19	165	0.51	0.57
179	0.39	0.18	172	0.51	0.59
186	0.40	0.21	186	0.51	0.61
207	0.44	0.23			
214	0.44	0.24			
235	0.45	0.26			
289	0.48	0.32			
372	0.53	0.41			

Table **C-3**: Expansion and mass gain results for WE-CPT prisms made with very highly reactive Jobe aggregate.

WE-CPT 38			WE-CPT 60		
Day	Length (% Change)	Mass (% Change)	Day	Length (% Change)	Mass (% Change)
0	0.00	0.00	0	0.00	0.00
7	0.01	-0.02	7	0.14	0.01
14	0.00	0.00	14	0.21	0.10
21	0.01	-0.01	21	0.28	0.14
28	0.01	0.00	28	0.30	0.19
35	0.04	0.01	35	0.32	0.20
42	0.07	0.02	42	0.34	0.25
49	0.10	0.04	49	0.35	0.26
56	0.12	0.05	56	0.36	0.29
63	0.15	0.06	63	0.37	0.37
70	0.16	0.07	70	0.38	0.40
88	0.21	0.11	88	0.39	0.46
95	0.22	0.05	95	0.39	0.52
102	0.25	0.14	102	0.40	0.58
109	0.26	0.13	109	0.40	0.64
123	0.28	0.13	123	0.40	0.70
130	0.30	0.13	130	0.41	0.75
151	0.33	0.14	151	0.40	0.83
158	0.35	0.18	158	0.41	0.85
179	0.36	0.20	179	0.41	0.87
233	0.40	0.21			
316	0.42	0.28			

Table **C-4**: Expansion and mass gain results for CPT prisms made with highly reactive Spratt aggregate.

CPT 38		
Day	Length	Mass
0	0.00	0.00
20	0.01	0.25
50	0.04	0.76
81	0.08	0.91
110	0.11	1.03
142	0.13	1.03
169	0.14	1.08
200	0.17	1.12
247	0.18	1.21
263	0.18	1.23
281	0.19	1.28
310	0.19	1.25
368	0.20	1.33

Table **C-5**: Expansion and mass gain results for S-CPT prisms made with highly reactive Spratt aggregate.

S-CPT 38			**S-CPT 60**		
Day	Length	Mass	Day	Length	Mass
0	0.00	0.00	0	0.00	0.00
7	0.00	0.02	7	0.00	0.00
14	0.00	0.01	14	0.01	0.03
21	-0.01	0.03	21	0.03	0.07
28	-0.01	0.05	28	0.03	0.08
35	0.00	0.07	35	0.04	0.14
42	0.00	0.07	42	0.04	0.15
49	0.01	0.09	71	0.07	0.32
71	0.05	0.12	78	0.07	0.36
78	0.06	0.16	85	0.07	0.39
85	0.06	0.15	92	0.07	0.44
92	0.07	0.16	106	0.08	0.49
106	0.07	0.17	127	0.08	0.59
127	0.09	0.18	134	0.08	0.62
134	0.09	0.25	155	0.09	0.70
155	0.10	0.23	209	0.09	0.91
209	0.11	0.31			
292	0.12	0.44			

Table **C-6**: Expansion and mass gain results for WE-CPT prisms made with highly reactive Spratt aggregate.

WE-CPT 38			**WE-CPT 60**		
Day	Length	Mass	Day	Length	Mass
0	0.00	0.00	0	0.00	0.00
3	-0.01	0.04	3	0.00	0.02
7	0.01	0.03	7	0.01	0.01
14	0.01	0.03	14	0.03	0.02
21	0.01	0.04	21	0.05	0.05
28	0.02	0.06	28	0.06	0.07
35	0.02	0.06	35	0.07	0.07
42	0.02	0.08	42	0.07	0.12
56	0.03	0.08	56	0.07	0.12
63	0.03	0.09	63	0.08	0.17
70	0.04	0.11	70	0.08	0.18
77	0.04	0.11	77	0.07	0.20
84	0.05	0.13	84	0.08	0.21
91	0.05	0.14	91	0.09	0.24
98	0.06	0.12	98	0.08	0.24
105	0.06	0.13	105	0.09	0.26
112	0.06	0.15	112	0.09	0.28
126	0.06	0.14	126	0.09	0.29
133	0.07	0.17	133	0.09	0.34
211	0.09	0.18	211	0.09	0.36
218	0.09	0.27	218	0.09	0.20
225	0.10	0.30	225	0.10	0.24
239	0.10	0.30	232	0.10	0.27
246	0.10	0.31	246	0.10	0.30
274	0.11	0.32	267	0.10	0.34
295	0.12	0.35			
349	0.12	0.36			
432	0.12	0.42			

Table **C-7**: Expansion and mass gain results for CPT prisms made with moderately reactive Tyrone River Sand aggregate.

CPT 38			**CPT 60**		
Day	Length	Mass	Day	Length	Mass
0	0.00	0.00	0	0.00	0.00
7	0.00	0.17	4	0.00	-0.20
36	0.01	0.41	8	0.00	-0.13
76	0.02	0.47	15	0.01	-0.08
114	0.02	0.46	19	0.01	-0.15
139	0.02	0.47	22	0.01	-0.20
169	0.03	0.50	26	0.01	-0.17
195	0.03	0.51	29	0.01	-0.17
226	0.04	0.53	33	0.01	-0.12
256	0.04	0.53	36	0.02	-0.09
287	0.05	0.58	40	0.02	-0.12
322	0.05	0.60	47	0.03	-0.09
350	0.06	0.63	50	0.03	-0.10
			53	0.03	-0.10
			59	0.03	0.00
			95	0.03	0.00
			102	0.04	0.00
			109	0.04	
			116	0.04	
			123	0.04	
			130	0.04	
			138	0.04	
			144	0.04	
			151	0.04	
			158	0.04	

Table **C-8**: Expansion and mass gain results for S-CPT prisms made with moderately reactive Tyrone River Sand aggregate.

S-CPT 38			**S-CPT 60**		
Day	Length	Mass	Day	Length	Mass
0	0.00	0.00	0	0.00	0.00
7	0.00	0.03	7	0.01	0.09
14	0.01	0.06	14	0.00	0.09
28	0.00	0.07	21	0.01	0.13
35	0.01	0.08	35	0.02	0.20
56	0.01	0.11	56	0.02	0.24
63	0.02	0.12	63	0.02	0.26
84	0.02	0.15	84	0.02	0.32
138	0.02	0.22	138	0.03	0.37
221	0.03	0.34	221	0.03	0.54

Table **C-9**: Expansion and mass gain results for WE-CPT prisms made with moderately reactive Tyrone River Sand aggregate.

WE-CPT 38			**WE-CPT 60**		
Day	Length	Mass	Day	Length	Mass
0	0.00	0.00	0	0.00	0.00
7	0.00	0.10	7	0.00	0.05
21	0.00	0.19	14	0.01	0.09
28	0.00	0.21	28	0.02	0.16
49	0.01	0.27	49	0.02	0.30
56	0.01	0.31	56	0.02	0.30
77	0.02	0.35	77	0.02	0.42
131	0.03	0.45	131	0.02	0.55
214	0.03	0.66	214	0.02	0.69

Table **C-10**: Expansion and mass gain results for CPT prisms made with moderately reactive Tyrone River Sand aggregate with 25% cement replacement with class F fly ash to mitigate ASR.

CPT 38			**CPT 60**		
Day	Length	Mass	Day	Length	Mass
0	0.00	0.00	0	0	0
7	0.00	0.10	7	0.00	0.12
21	0.00	0.17	14	0.00	0.15
28	-0.01	0.17	28	0.00	0.17
49	0.00	0.21	49	0.00	0.22
56	0.00	0.18	56	0.00	0.22
77	0.00	0.20	77	0.00	0.19
131	0.00	0.24	131	0.01	0.29
214	0.00	0.27	214	0.02	0.34

Table **C-11**: Expansion and mass gain results for S-CPT prisms made with moderately reactive Tyrone River Sand aggregate with 25% cement replacement with class F fly ash to mitigate ASR.

S-CPT 38			**S-CPT 60**		
Day	Length	Mass	Day	Length	Mass
0	0.00	0.00	0	0.00	0.00
14	0.00	0.02	7	0.00	0.00
21	0.00	0.03	21	0.00	0.03
42	0.00	0.05	42	0.00	0.08
49	0.00	0.05	49	0.00	0.13
70	0.00	0.05	70	0.00	0.23
124	0.00	0.07	124	0.00	0.34
207	0.00	0.14	207	0.00	0.44

Table **C-12**: Expansion and mass gain results for WE-CPT prisms made with moderately reactive Tyrone River Sand aggregate with 25% cement replacement with class F fly ash to mitigate ASR.

WE-CPT 38			**WE-CPT 60**		
Day	Length	Mass	Day	Length	Mass
0	0.00	0.00	0	0.00	0.00
14	0.00	0.09	7	0.01	-0.01
21	0.00	0.11	21	0.01	0.08
42	0.01	0.15	42	0.01	0.12
49	0.01	0.18	49	0.02	0.15
70	0.01	0.19	70	0.01	0.17
124	0.01	0.24	124	0.02	0.25
207	0.01	0.28	207	0.02	0.35

Table **C-13**: Relative humidity results for ASR performance tests.

CPT 38		**CPT 60**		**S-CPT 38**		**S-CPT 60**		**WE-CPT 38**		**WE-CPT 60**	
Day	RH	Day	RH	Day	RH	Day	RH	Day	RH	Day	RH
7	92.6	7	89.4	7	90.9	7	88.4	7	93.1	7	88.3
14	93	14	88.3	14	90.5	49	89.1	14	92.8	14	88.3
21	93.4	21	86.8	21	90.7	64	88.2	21	92.7	21	87.6
28	93.4	28	86.2	28	90.6	71	86.7	28	93.5	28	87
35	93.3	35	85.4	35	93.6	78	88.7	35	93.1	35	86.7
42	95.1	42	84.7	42	92.1	85	86	42	92.7	42	86.5
49	92	49	85.6	49	91.3	92	84.7	49	93.1	49	86.8
84	91.6	126	87	71	91.7	127	88.8	56	94.4	56	86.6
98	93.8	133	88.3	78	90.9	209	89.3	63	93.5	63	88.2
119	90.2	182	89.5	85	89.9			70	92.1	70	88.2
126	91.9			106	88.5			88	91.1	88	85.7
133	91.2			127	91.6			95	91.4	95	86.9
140	89.9			134	92.1			102	90.8	102	85.3
161	89.3			188	94.1			109	90.8	109	86
182	89.8			292	94.3			130	89	123	85.2
189	91.6							151	91.2	130	89
243	94.7							158	88.8	151	90
347	95.3							212	94.9	158	88
								316	93.6	179	89.6